Miner Petrol
DOI 10.1007/s00710-011-0149-7

ORIGINAL PAPER

Geochemistry of microgranular enclaves in Aligoodarz Jurassic arc pluton, western Iran: implications for enclave generation by rapid crystallization of cogenetic granitoid magma

Amir Esna-Ashari · Jamshid Hassanzadeh · Mohammad-Vali Valizadeh

Received: 24 August 2010 / Accepted: 29 March 2011

Abstract Microgranular enclaves are common in the Jurassic Aligoodarz granitoids of western Iran. Enclaves Enclosed in Granodiorite (EEG) and Enclaves Enclosed in Tonalite (EET) are different but they overlap their hosts on variation diagrams. The EEG is compositionally intermediate between tonalite and granodiorite. Mixing between tonalitic and granodioritic magmas and fractional crystallization are two models examined as the origin of the EEG. Field, textural, mineralogical and chemical observations suggest that chemical equilibration, common in magma mixing, was not attained between the EEG and its host. This, together with other observations does not support magma mixing as a mechanism for forming the EEG. Alternatively, excessive nucleation of biotite ± Fe-Ti-oxides ± amphibole by rapid cooling at borders of a shallow magma chamber and later fragmentation and dispersal by dynamic arc plutonism best explains the EEG. However, channeling of a new magma into the nearly solid tonalitic host explains formation of the EET.

Introduction

A common feature of calc-alkaline granitoids is enclosing abundant Microgranular Enclaves (ME) (Didier and Barbarin 1991). The study of ME in granitoid rocks has a long history (Phillips 1880; Pabst 1928; Cloos 1936; Didier 1973; Vernon 1983, 1990), and has brought about several hypotheses regarding the origin of the ME which reflects the complexity of enclave-forming processes. One major debating issue in such studies is identification of the parental magmas of the ME. A widely accepted view for the genesis and evolution of ME is that they are resulted from mixing or mingling of mafic and crustal felsic magmas (Vernon 1984; Frost and Mahood 1987; Dorais et al. 1990; Blundy and Sparks 1992; Wiebe et al. 1997; Perugini et al. 2003; Barbarin 2005; Feeley et al. 2008). Advocates of magma mixing attribute the compositional similarities between enclaves and host rocks to varying degrees of chemical equilibration and diffusional exchange between the coexisting magmas during slow cooling (Pin et al. 1990; Allen 1991; Holden et al. 1991).

An alternative view named the "Restite Model" considers the origin of ME as refractory solid residues of partial melting from the source region (White and Chappell 1977; Chappell 1978; Chen et al. 1989; Chappell 1996; White et al. 1999; Chappell et al. 2000). But Barbarin and Didier (1991) and Vernon (1983, 1991) have challenged the "Restite Model" by making distinctions between restites and ME based on textural, mineralogical and chemical observations.

A fundamentally different hypothesis known as "Cognate Model" considers accumulation of early crystallized minerals from the magma or a more mafic cogenetic melt and trapped interstitial liquids for the origin of ME (Phillips et al. 1981; Clemens and Wall 1984, 1988; Dodge and Kistler 1990; Fershtater and Borodina 1977, 1991; Dahlquist 2002; Ilbeyli and Pearce 2005). Similar geochemistry and isotopic characteristics of

Editorial handling: R. Abart

A. Esna-Ashari · M.-V. Valizadeh
School of Geology, College of Science, University of Tehran,
Tehran, Iran

J. Hassanzadeh (✉)
Tectonics Observatory, Division of Geological and Planetary
Sciences, California Institute of Technology,
Pasadena, CA, USA
e-mail: Jamshid@caltech.edu

Published online: 13 April 2011

the ME and their host rocks are easily interpretable in terms of this hypothesis. Under “Cognate Model” three slightly different mechanisms have been proposed as: 1- cumulate clots (Dodge and Kistler 1990; Dahlquist 2002), 2- disrupted chilled margins (Donaire et al. 2005), and 3- disrupted cumulate assemblages (Bébien 1991; Platevoet and Bonin 1991).

The purpose of this study is to determine the petrologic properties of the enclaves within the Aligoodarz granitoids and explain their genetic link with the host rocks using field relationships, petrography, whole-rock geochemistry, and mineral chemistry. Our data indicates that there are two types of ME in this area. One type is resulted from breakup of a possibly tonalitic chilled margin and the subsequent dispersal in the granodioritic host magma. The other type of enclaves formed as composite or fragmented dikes when a new magma injected the largely crystallized host tonalite. Mingling/mixing of the intruded magma with its host was not very extensive but chemical equilibration modified the composition of the enclaves to some extent.

Geological setting

Aligoodarz granitoid is a range-parallel pluton with surface area of ~80 km^2 intruding late Triassic-Jurassic low grade metapelites north of the town of Aligoodarz in the northwest trending Sanandaj-Sirjan Zone (SSZ) of western Iran (Fig. 1). The SSZ is a 1,500 km long, 200 km wide sector in the Alpine-Himalayan orogenic system which runs parallel to the Main Zagros Thrust, and represents the northern margin of the Neotethyan ocean in the Mesozoic and Cenozoic time (Sengör 1990). In the Mesozoic, the SSZ was an active Andean-like margin with typical calc-alkaline magmatic activity (Berberian and King 1981). Different Mesozoic ages have been reported for other granitoids of this zone (e.g. Valizadeh and Cantagrel 1975; Masoudi 1997; Ahmadi Khalaji et al. 2007; Shahbazi et al. 2010).

Khorheh (K) and Mollataleb (M) are two separate outcrops of the granitoid body surrounded by relatively thin contact aureole (Fig. 1b). U-Pb zircon dating has yielded ages of 172 Ma for the tonalite and 172 Ma and 182 Ma for the granodiorite at M and K, respectively (Esna-Ashari et al. 2009).

Field relation and petrography

Classification of the investigated granitoids and their enclaves are shown on the QAP diagram of Streckeisen (1976) (Fig. 2a). This classification is based on the modal abundance of minerals presented in Table 1. According to this nomenclature, granodiorite, tonalite and granite are the main rock types in the studied area (Fig. 1b). Contacts between these units are intrusive and generally sharp. Granite is the most evolved phase and occurs as fine-grained leucocratic dikes and small stocks intruding the granodiorite. Microgranular enclaves are common in tonalite and granodiorite but absent in granite. Field relation, petrography and the way of formation of the Enclaves Enclosed in Tonalite (EET) are different from the Enclaves Enclosed in Granodiorite (EEG) and will be discussed in the following subsections.

Granite

Granite is light in color and is mostly fine-grained. It mainly consists of quartz, K-feldspars and plagioclase (Table 1). Muscovite, biotite, tourmaline, apatite and garnet are accessory minerals. Garnet occurs as fine anhedral crystals. In some locations tourmaline is very abundant and forms orbicular aggregates. Alteration of biotite to chlorite and feldspar to sericite are common.

Granodiorite and their enclaves

The granodiorite is medium- to coarse-grained with hypidiomorphic texture and is the main rock type in the area. Plagioclase, quartz, biotite and K-feldspar are the major minerals of the granodiorite (Table 1). Accessory minerals include zircon, Fe-Ti-oxides, tourmaline and apatite. Biotite is highly pleochroic and occurs as euhedral to subhedral flakes showing slight alteration to muscovite and/or titanite and Fe-Ti oxides. K-feldspars include orthoclase and microcline. Plagioclase (An_{35-55}) forms rectangular to subhedral laths with variable degrees of sericitization.

The EEG is distributed throughout the granodiorite outcrops with sizes ranging from centimeters to tens of centimeters. Although conspicuous in most outcrops they are more common in Mollataleb than in Khorheh (Fig. 1b). Enclaves are angular, ellipsoidal or lenticular in shape (Fig. 3a). Irregular patches of the host magma are injected into some enclaves (Fig. 3b). The injected granodiorite has texture and mineral content similar to those of the granodiorite enclosing the enclave and the contact between the two is sharp. No chilled margin has been observed in any enclave.

Petrographically the EEG has many similarities to the host granodiorite, but show microgranular texture (Fig. 4a, b) and are commonly tonalitic in composition. Textures vary from equigranular fine-grained to porphyritic. The grains are often euhedral to subhedral and the least altered enclaves contain plagioclase, quartz, biotite ± amphibole with minor orthoclase (Table 1). Minerals present in the

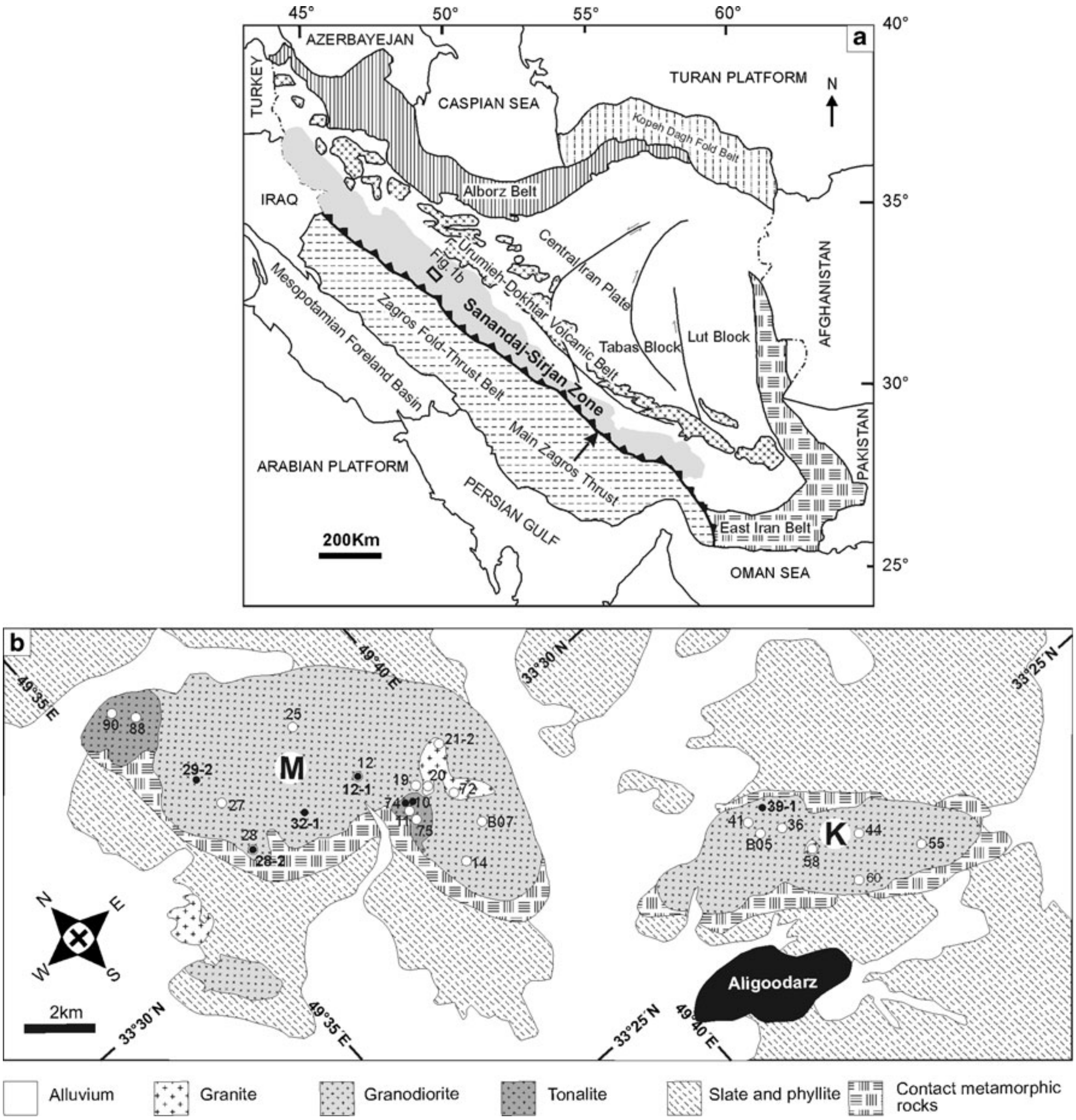

Fig. 1 **a**) Generalized tectonic map of Iran based on geological maps of Ruttner and Stöcklin (1967) and Alavi (1991). **b**) Simplified geological map of the Aligoodarz granitoids. Mollataleb (M) and Khorheh (K) are the two main separate outcrops. *Open and filled circles* respectively show the locations of collected granitoids and their enclaves discussed in the text

enclaves are generally the same as those of the enclosing granodiorite and the difference is in their abundances. However, some enclaves contain abundant amphibole not seen in the host. EEG generally has higher modal contents of biotite than the host granodiorite and K-feldspar is less abundant or absent in the enclaves. Zircon, acicular apatite, sphene and opaques are the accessory phases. Chlorite and sericite are the secondary phases after biotite and feldspar, respectively. In enclaves with porphyritic textures, plagioclase phenocrysts are dominant and occur in a fine-grained groundmass composed of plagioclase, biotite, quartz and amphibole. Plagioclase and amphibole grains are often elongated. Zircon is commonly included in biotite (Fig. 4a) but also present as inclusions in other minerals. Plagioclases (An_{32-80}) show patchy zoning and are characterized by resorbed zones in the cores which are filled by more sodic plagiocalses or quartz. The corroded patchy zoning interiors of some plagioclase phenocrysts show late overgrowths (Fig. 4b). In some cases the late overgrowths are oscillatory zoned. Quartz occurs as poikilitic crystal enclosing fine-grained euhedral plagioclase and biotite in some enclaves (Fig. 4a).

Along the contact of granodiorite and tonalite a different kind of enclaves occur in the granodiorite (Fig. 3c). These

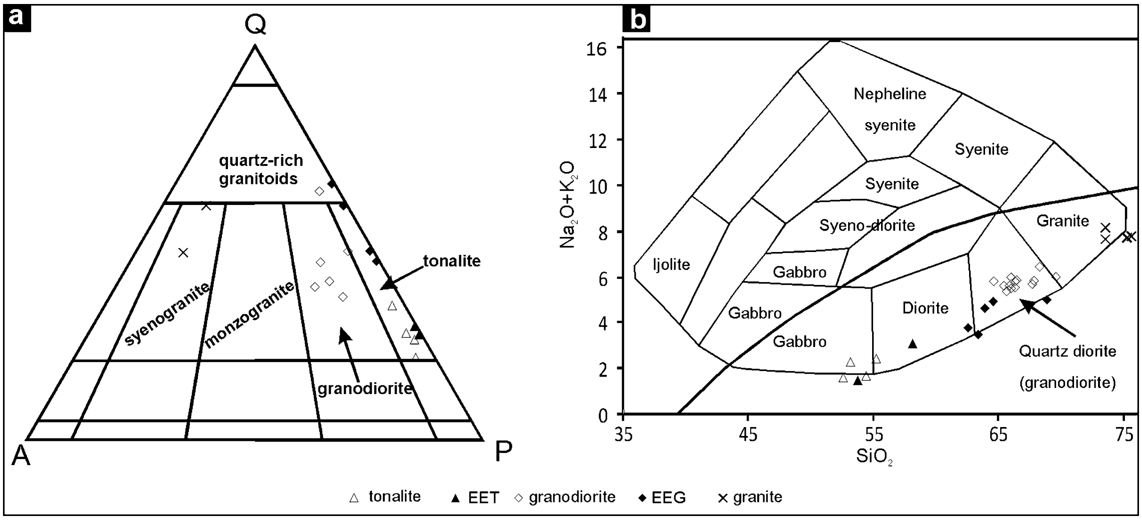

Fig. 2 **a**) QAP diagram of granitoids and their enclosed enclaves. **b**) Classification of the enclaves and their host rocks on the basis of TAS diagram

enclaves are closely spaced and seem to be fragments of the tonalite caught in the intruding granodiorite. These enclaves are coarse grained and petrographically different from the aforementioned EEG but similar to the adjacent tonalite (Fig. 4c). They exhibit angular forms (Fig. 3c) which indicate their disrupted nature and closeness to the source region. So, they can be referred to as xenoliths entered the host magma after disruption of tonalite. They also indicate earlier crystallization of tonalite relative to granodiorite. Due to the differences discussed above we do not group the latter with the EEG.

Tonalite and their enclaves

Tonalite is fine- to medium-grained and differ from other rocks by their higher color index and abundant amphibole. They contain lower modal quartz and higher modal mafic minerals compared with other rock types. Amphibole, biotite, quartz and plagioclase are the major minerals (Table 1). Minor phases include zircon, apatite and Fe-Ti-oxides. The rock texture is hypidiomorphic. Amphibole grains occur either as prismatic crystals or as irregular grains. Plagioclase ($An_{47–90}$) occurs as zoned euhedral to

Table 1 Representative modal analyses of enclaves and their host rocks

Rock type		sample	Pl	Bt	Qtz	Kfs	Amph	Px
Tonalite		AL11	45.9	13.0	16.0	1.4	23.7	0.0
		AL75	31.9	24.5	17.3	1.5	24.9	0.0
		AL88	41.3	8.2	16.1	1.8	32.6	0.0
		AL90	24.6	4.2	6.6	1.5	63.2	0.0
Granodiorite		B07	42.3	17.0	30.0	10.7	0.0	0.0
		AL27	26.4	19.3	50.6	3.6	0.0	0.0
		AL19	36.0	22.5	37.0	4.4	0.0	0.0
		B05	38.0	17.7	33.1	11.2	0.0	0.0
		AL44	34.4	18.0	37.0	10.7	0.0	0.0
		AL55	35.7	18.6	31.5	14.3	0.0	0.0
Granite		AL21-2	10.4	<1	47.5	42.1	0.0	0.0
		AL20	9.1	2.4	58.3	30.1	0.0	0.0
EEG	Amphibole-bearing	AL29-2	20.4	34.1	38.9	<2	6.2	0.0
		AL12-1	25.4	30.4	38.1	<2	5.5	0.0
	Amphibole-free	AL39-1	40.3	25.1	33.8	<2	0.0	0.0
		AL28-2	39.7	22.6	37.1	<2	0.0	0.0
EET		AL74	48.3	14.9	18.1	<1	4.8	13.8
		AL10	46.7	12.5	19.0	<1	3.4	18.1

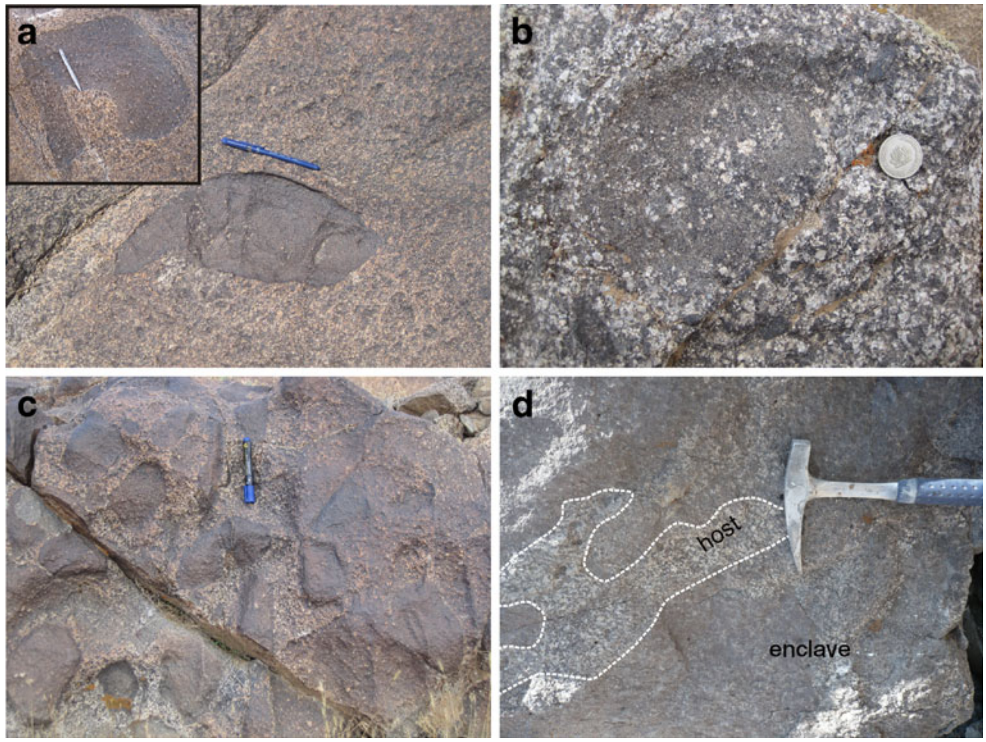

Fig. 3 Various types of enclaves in the Aligoodarz granitoids: **a**) microgranular enclaves enclosed in granodiorite (EEG), characterized by angular shapes, absence of chilled margin and lack of compositional zoning; **b**) intrusion of host granodioritic magma into EEG. The contact between the intruded magma and the host enclave is generally sharp; i.e., no transitional zone; **c**) Swarms of mafic enclaves as disrupted fragments of tonalite which are enclosed in granodiorite in places close to the contact with tonalite; **d**) amorphous microgranular enclaves enclosed in tonalite (EET) with enclave-host intertwined relationship as a result of late surge of magma into the nearly-solid tonalitic host. The tonalitic host is delineated by dashed line

subhedral laths and commonly shows oscillatory or normal concentric zoning (Fig. 4e). Near the contact with the enclaves, plagioclases show patchy zoning with complex anorthite distribution discussed in the following.

Rare but large microgranular enclave clusters occur in tonalite. Two clusters of such enclaves, few meters in diameter, were examined. General microscopic and macroscopic differences between this type of enclaves and the EEG are summarized in Table 2 and will be discussed more in the following sections. The EET is tonalitic in composition and display amorphous shapes. Contact of the enclaves with the host tonalite is generally sharp. Interfingering with the host rock is common and apophyses of the host penetrate the enclaves (Fig. 3d). The enclaves are finer-grained than the host rock and show igneous, non-oriented, porphyritic texture. In terms of major minerals the EET is similar to their host tonalite excluding the absence of pyroxenes in the latter. Pyroxene is generally rimmed by amphibole. Plagioclase, pyroxene, biotite, quartz and amphibole are major minerals. Plagioclase is present as both phenocryst and groundmass phase with An_{45-88}. Large plagioclases show complex zoning. Partially resorbed cores of large plagioclases show patchy zoning. Rims and resorbed zones of the cores are more albite rich (Fig. 4f). Such large plagioclases are also abundant in the host especially near the contact with the enclaves (Fig. 4d). By increasing distance from the enclaves the abundance of this type of plagioclase decreases.

Analytical methods

Out of 150 samples from the host and 60 samples from the enclaves were collected from different localities, 140 samples were selected for optical microscopy studies and 28 for whole rock geochemical analysis. Locations of the selected samples for chemical analyses are shown in Fig. 1b. Samples of 2–3 kg from the host rocks and 1–2 kg from the enclaves were crushed by jaw-crusher and then powdered in a (tungsten-carbide) ring pulverizer. Results of whole rock geochemical analyses are presented in Table 3. Major element concentrations were analyzed by Inductively Coupled Plasma Atomic Emission Spectrometry (ICP-AES) with a detection limit of 0.01%. Trace elements were analyzed by Inductively Coupled Plasma-Mass Spectrometry (ICP-MS) with detection limit of 0.01 to 10 ppm following lithium metaborate fusion method. Relative standard deviations are better than ±4% for most elements. All whole rock analyses were carried out at ALS Chemex laboratories in Vancouver, Canada. Details of the analytical procedures are accessible at www.alschemex.com.

Chemical compositions of minerals were determined on JEOL JXA-8200 electron microprobe at California Institute of Technology using a focused electron beam with an accelerating voltage of 15 kV and a beam current of 25 nA. The data were reduced using CITZAF algorithm (Armstrong 1988). Representative mineral compositions are tabulated in Table 4.

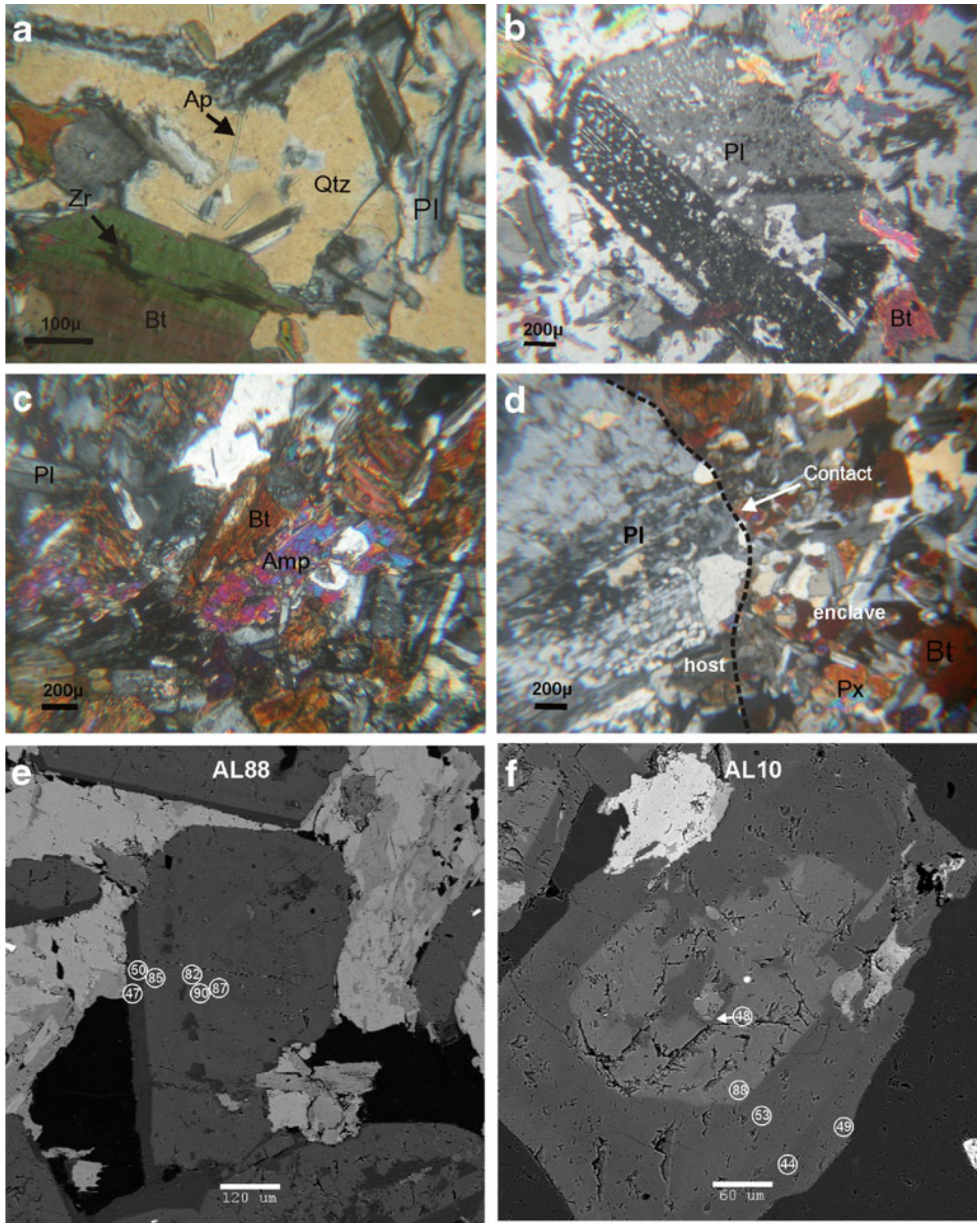

Fig. 4 Photomicrographs of enclaves in crossed polars (**a**–**d**); and back scatter electron images (BSE) of plagioclases in tonalite (**e**) and its enclave (**f**). **a**) Photomicrograph of an enclave enclosed in granodiorite (EEG). Crystals of plagioclase, apatite and biotite are poikilitically enclosed in a large grain of quartz; with zircon included in biotite; **b**) Plagioclase phenocryst showing rounding and internal corrosion by dissolution in the magma. The corroded portions were filled with more sodic plagioclase which also rims the grain; **c**) a cumulate enclave within granodiorite from near tonalite-granodiorite contact displaying larger grain size compared to the EEG shown in Fig. 4a; **d**) photomicrograph of the contact of EET with the host. Large plagioclase crystals of the host show internal resorbed zones as the result of disequilibrium induced by intrusion of the enclave magma. Ap: apatite; Qtz: quartz; Zr: zircon; Bt: biotite; Pl: plagioclase; Amp: amphibole; Px: pyroxene. In the BSE images *circled numbers* represent anorthite contents

Geochemistry

Whole rock geochemistry

Table 3 presents whole rock major and trace element data for representative samples of enclaves, their host rocks and granite. Figure 2b shows nomenclature of our samples on Total Alkalis-Silica diagram. Granites, although devoid of enclaves, are included to investigate possible links with the other two rock groups. The EEG is generally more enriched in compatible elements like CaO, MgO, Fe_2O_3 and Co compared to their hosts. The ME, their hosts and granite form a relatively continuous suite in the Harker diagrams, and show linear trends, with decreasing Fe_2O_3, CaO, MgO, MnO, V and Co and increasing K_2O, Rb and Ta relative to SiO_2 (Fig. 5). Correlation of Ba and Zr with SiO_2 is different and a remarkable Ba- and Zr-depletion in granite gives rise to a peculiar curvilinear trend also observed in Boggy Plain Supersuite granitoids (Chappell 1996). Chemical gaps occur between granodiorite, tonalite and granite. Tonalite has intermediate (SiO_2~52–55%) but granodiorite and granite have felsic compositions (SiO_2~65–68% and 73–76% respectively). In addition to differences in modal content of minerals and petrographic features of the EET and EEG, chemistry of these two types of enclaves is also different as the range of SiO_2 content for EET and EEG is 54–58% and 63–69%, respectively.

In most Harker diagrams, the EEG follows the general trend of all other samples. However, behavior of K_2O and Ba for EEG is different from the general trend. Such

Table 2 Macroscopic and microscopic differences between Enclaves Enclosed in Granodiorite (EEG) and Enclaves Enclosed in Tonalite (EET)

	Observation	EEG	EET
Macroscopic	Abundance	Ubiquitous	Rare
	Size	Few centimeters to tens of centimeters	Few meters
	Shape	Angular to ellipsoidal and lenticular	amorphous
	Cross-cutting relations	Host magma cross-cuts the enclave	Enclave magma cross-cuts the host
	Chilled margin	None	None
Microscopic	Rock texture	Equigranular, fine-grained to porphyritic	porphyritic
	Minerals that are present in the enclave but absent in the host	amphibole	pyroxene
	Mineral exchange between enclave and host	None	Plagioclase migration from the host into the enclave
	Plagioclase texture	Patchy zoning as the result of decompression	Patchy zoning resulted from disequilibrium caused by injection of new magma
	Textural changes of the host in the contact zone	None	Plagioclases with patchy zoning are concentrated in the contact zones

different behaviors are better shown when compatible elements Fe_2O_3, MgO, CaO, MnO and Co are plotted against K_2O (Fig. 6a). Variation trends for the EEG are different from the trends displayed by other samples. Such distinct variation trends for the EEG are also observed for Ba when it is plotted against the above-mentioned compatible elements (not shown). Two of the EEG samples with the lowest SiO_2 but the highest K_2O (Table 3) contain amphiboles and are characterized by highest mafic content; the remaining three EEG samples lack amphibole and contain less biotite (Table 1).

Figure 6b shows variation trends of some elements against MgO and reveals critical chemical differences among the various groups of rocks in this study and they include: 1- the tonalites are distinct from the remaining samples, 2-the EEG are close to their host rocks and different from the tonalite, 3- some of the EEG are more enriched in TiO_2 and HREE in comparison with tonalite and granodiorite. HREE enrichment of the EEG is also obvious in their chondrite normalized REE patterns shown in Fig. 7a–b. Generally the enclaves exhibit similar patterns, and similar LREE/HREE ratios relative to their respective hosts but amphibole bearing EEG are more enriched in HREE than their hosts.

Mineral chemistry

Microprobe analyses of plagioclase, biotite and amphibole of selected enclaves and host rocks are presented in Table 4. A comparison of enclave-host mineral chemistry follows. Plagioclases of EEG are more enriched in anorthite than their corresponding host; in contrast, the range of anorthite content of plagioclases in EET and their host tonalite are similar. Plagioclases in both the EEG and EET show complex inner structure and compositional zoning. Many large plagioclases show patchy zoning which consists of irregular resorbed cores, the corroded portions having been filled and surrounded by plagioclases with lower or similar anorthite contents to their cores (Fig. 4b and f). Oscillatory zoning is also common. Some plagioclases show regular concentric normal zoning.

Plagioclases with patchy zoning are not uniformly distributed in tonalite and they are concentrated in areas close to the contact with enclaves (Fig. 4d). Such grains also occur in EET as phenocrysts. Figure 4f shows a phenocryst within the enclave AL10 which is characterized by a typical resorbed core with irregular embayments. The resorbed zones are filled with albite-rich plagioclase. The plagioclase rimming the calcic core is compositionally similar to the filled resorbed holes. Note that the boundaries between different zones are straight and sharp.

Biotites in amphibole-free EEG are compositionally similar to biotites of the enclosing host but those in amphibole-bearing EEG are chemically different from the ones in the host (Table 4; Fig. 7c). The same differences exist in mineral composition of EET and the host tonalite. Biotite is present in both the EET and their host tonalite but their chemical compositions are different (Fig. 7c). Chemical composition of biotites in each group of host rocks and their enclaves are displayed in TiO_2 vs. Mg# diagram shown in Fig. 7c. Mg# of the biotites are not the same but amphibole-free EEG are compositionally similar to their host.

Discussion

Many mechanisms have been proposed for the genesis of the ME. In many cases determining the exact mechanism

Table 3 Chemical analyses for granite, granodiorite, tonalite and microgranular enclaves

	Tonalite				Granodiorite													Granite				EEG					EET	
Sample	AL 75	AL 88	AL 90	AL 11	AL 60	AL 36	B 05	AL 41	AL 44	AL 55	B 07	AL 12	AL 14	AL 19	AL 25	AL 27	AL 28	AL 20	AL 21 -2	AL 58	AL 72	AL 12 -1	AL 28 -2	AL 29 -2	AL 32 -1	AL 39 -1	AL10	AL74
wt%																												
SiO_2	55.2	53.2	52.6	54.4	66.5	65.4	67.9	66.3	66.3	64.6	66.0	65.9	67.7	65.6	66.0	66.0	68.3	75.6	73.5	73.5	75.2	62.6	68.9	63.4	64.6	63.9	58.1	53.7
Al_2O_3	15.3	18.3	12.4	17.1	15.0	15.6	14.9	15.6	15.6	16.0	15.8	15.4	14.8	15.8	15.6	15.1	14.3	13.7	13.9	14.6	13.9	15.7	14.4	14.9	15.0	15.2	18.1	17.9
Fe_2O_3	9.3	9.8	8.9	7.9	4.9	5.4	5.4	5.6	5.3	5.9	5.1	5.7	5.0	5.1	5.1	5.0	3.9	1.0	1.0	1.5	1.1	7.4	5.1	6.2	6.1	6.6	8.3	9.7
CaO	6.3	8.5	9.5	8.0	2.7	3.4	3.2	3.2	3.2	3.4	3.3	3.6	3.2	3.6	3.2	3.2	2.3	0.7	0.6	1.1	0.6	5.7	3.2	5.5	3.6	4.0	6.9	8.9
MgO	8.1	5.8	12.7	7.5	1.4	1.4	1.4	1.7	1.4	1.7	1.5	1.8	1.5	1.6	1.6	1.6	1.0	0.2	0.1	0.2	0.2	2.8	1.2	3.5	1.8	1.8	4.0	5.8
Na_2O	0.9	1.3	1.1	1.0	2.4	2.5	2.4	2.4	2.5	2.5	2.7	2.5	2.6	2.6	2.5	2.3	2.4	3.0	3.0	3.1	3.4	1.1	3.0	1.1	2.6	2.3	2.4	1.0
K_2O	1.5	1.0	0.6	0.7	3.5	3.1	3.4	3.2	3.3	3.4	3.3	3.1	3.0	2.7	3.2	3.1	4.2	4.7	5.2	4.5	4.3	2.7	1.8	2.4	2.3	2.3	0.8	0.6
TiO_2	0.61	0.58	0.53	0.37	0.52	0.58	0.64	0.64	0.55	0.59	0.63	0.72	0.65	0.59	0.60	0.60	0.46	0.05	0.03	0.06	0.05	0.80	0.59	0.47	0.89	1.06	0.39	0.40
MnO	0.18	0.19	0.18	0.14	0.10	0.11	0.10	0.11	0.11	0.10	0.10	0.11	0.09	0.10	0.10	0.09	0.07	0.06	0.02	0.03	0.03	0.15	0.09	0.13	0.11	0.11	0.16	0.19
P_2O_5	0.08	0.18	0.08	nd	0.15	0.15	0.14	0.15	0.15	0.14	0.12	0.13	0.14	0.14	0.17	0.20	0.13	0.13	0.17	0.18	0.20	0.13	0.17	0.10	0.16	0.18	0.16	0.17
LOI	2.42	1.36	1.55	1.56	1.47	1.48	1.08	0.49	1.28	1.64	1.28	0.98	1.44	0.88	0.70	1.09	0.96	0.79	0.79	1.17	0.89	1.08	0.76	1.17	1.38	1.06	0.1	0.00
Total	99.9	100.2	99.9	98.7	98.6	99.0	100.6	99.3	99.6	99.8	99.8	99.9	100.2	98.7	98.6	98.3	97.9	99.9	98.3	100.0	99.8	100.1	99.3	98.9	98.6	98.4	99.3	98.4
ppm																												
Ba	184	121	69	111	356	329	389	347	345	399	359	350	398	291	332	393	401	103	67	406	67	295	113.5	237	156	163	143	122
Ce	26.1	27.6	18.6	25.4	75.8	71.8	72.7	73.0	63.0	56.5	70.2	74.5	76.6	76.9	72.5	81.5	59.4	20.4	14.2	27.0	13.7	58.1	54.5	52.8	66.4	63.5	46	24.5
Co	34.0	31.3	43.7	34.4	9.9	10.1	10.3	12.9	10.4	12.0	11.5	12.8	10.1	11.8	11.3	12.0	8.1	1.2	1.8	1.8	1.0	17.8	9.7	18.5	13.8	13.9	22.8	33.1
Cr	690	170	1240	580	50	40	40	60	40	60	50	70	50	60	60	60	30	10	10	10	10	80	10	180	50	50	130	260
Cs	4.9	8.7	2.0	2.8	8.0	7.3	6.6	8.5	9.0	7.1	9.3	7.6	6.7	7.9	16.4	8.4	6.3	4.4	4.9	4.9	6.2	6.8	5.7	9.3	6.1	6.3	1.7	1.8
Dy	2.5	2.4	2.7	2.2	4.8	4.5	4.7	5.3	5.0	3.8	5.4	5.0	5.0	4.8	4.8	5.6	5.4	3.0	1.8	1.3	1.8	5.1	5.3	6.3	4.6	5.8	3.1	2.5
Er	1.6	1.5	1.6	1.5	2.6	2.6	2.9	3.1	2.9	2.2	3.2	3.1	2.9	2.6	2.6	3.2	3.4	2.0	1.1	0.5	1.1	3.4	2.8	4.4	2.1	3.3	1.9	1.6
Eu	0.7	0.8	0.6	0.7	1.0	1.1	1.0	1.1	1.0	1.0	1.1	1.1	1.1	1.2	1.1	1.2	1.0	0.3	0.2	0.8	0.1	1.0	0.7	0.7	1.0	0.9	1.2	0.9
Ga	16.8	19.4	12.4	17.3	19.5	20.0	19.3	19.7	19.8	20.3	21.1	20.6	20.1	19.9	19.9	21.2	16.8	13.4	15.0	20.2	16.9	19.8	19.6	16.5	19.5	19.8	19.0	18.7
Gd	2.5	2.6	2.3	2.4	6.4	5.9	5.8	6.4	5.6	4.6	6.2	6.3	6.4	6.5	6.2	7.0	5.6	2.1	1.5	2.7	1.3	5.3	6.1	5.4	6.4	6.3	3.7	2.6
Hf	1.5	1.7	2.2	1.4	5.8	5.3	4.8	5.7	5.0	5.6	5.1	5.7	5.3	5.4	5.3	5.3	4.3	1.9	1.6	2.5	1.5	4.7	4.1	4.3	4.5	5.0	2.1	1.6
Ho	0.5	0.5	0.6	0.5	0.9	0.9	0.9	1.1	1.0	0.7	1.1	1.0	1.0	0.9	0.9	1.1	1.1	0.7	0.4	0.2	0.4	1.1	1.0	1.4	0.8	1.1	0.7	0.5
La	13.3	13.7	8.6	11.8	37.8	35.9	34.9	36.1	30.9	27.9	33.3	35.6	37.1	37.8	35.5	40.2	29.3	10.3	7.4	12.9	7.3	28.6	26.8	25.8	32.0	31.0	22.5	11.4
Lu	0.2	0.2	0.3	0.2	0.4	0.4	0.4	0.4	0.4	0.3	0.4	0.4	0.4	0.4	0.4	0.4	0.5	0.4	0.2	0.1	0.2	0.5	0.3	0.7	0.3	0.4	0.3	0.3
Nb	7.4	6.0	4.2	5.6	13.4	13.6	13.4	13.3	13.3	13.5	12.3	13.2	12.7	13.0	13.2	13.5	10.4	6.0	7.4	13.7	5.2	10.7	12.0	9.3	12.9	13.4	7.6	4.7
Nd	11.7	12.6	10.0	10.9	33.1	31.1	30.5	32.2	27.4	24.4	30.2	31.9	33.1	33.5	31.1	35.1	25.8	7.7	5.4	12.5	4.9	25.2	25.0	23.3	30.0	28.8	18.8	11.2
Ni	43	28	111	48	17	14	16	20	13	15	18	23	16	21	20	20	11	nd	nd	nd	nd	10	8	36	13	10	16	44
Pr	3.1	3.3	2.4	2.9	9.0	8.5	8.5	8.7	7.2	6.6	8.3	8.6	8.9	8.9	8.3	9.4	7.0	2.3	1.6	3.3	1.5	6.9	6.6	6.3	7.8	7.6	5.2	2.9
Rb	70	45	23	35	167	140	149	141	147	152	151	143	132	130	148	148	151	138	174	166	236	110	124	96	137	137	32	30
Sm	2.5	2.6	2.4	2.3	6.7	6.4	6.1	6.5	5.6	5.0	6.2	6.5	6.6	6.7	6.3	7.1	5.6	1.9	1.4	3.4	1.2	5.3	5.8	5.2	6.2	6.2	4.0	2.4
Sn	1	1	1	1	6	3	3	3	3	3	3	3	3	3	4	3	2	5	6	3	5	1	2	2	2	1	1	
Sr	99	153	136	126	121	140	153	124	134	167	125	126	134	138	124	136	107	42	35	146	29	152	90	99	112	112	159	173
Ta	0.40	0.40	0.30	0.40	1.10	1.00	1.10	1.00	1.00	1.00	1.10	1.10	1.10	1.00	1.00	1.00	0.80	1.20	2.10	1.30	1.50	0.90	0.80	0.80	0.90	1.00	0.40	0.30
Tb	0.40	0.42	0.43	0.37	0.90	0.83	0.87	0.94	0.87	0.67	0.95	0.91	0.92	0.89	0.91	1.01	0.93	0.45	0.29	0.33	0.27	0.84	0.94	0.95	0.90	0.98	0.54	0.40
Th	3.8	4.2	2.5	4.2	15.1	13.3	14.4	14.3	13.1	13.0	13.9	14.8	15.2	13.5	13.3	15.3	11.8	8.4	6.2	5.6	5.0	10.4	10.5	10.8	12.2	10.3	6.6	2.6
Tm	0.25	0.22	0.26	0.20	0.36	0.36	0.39	0.45	0.42	0.31	0.45	0.43	0.39	0.37	0.38	0.47	0.47	0.34	0.18	0.07	0.18	0.51	0.35	0.65	0.27	0.45	0.31	0.25

U	0.85	0.85	0.53	0.66	1.84	1.63	1.95	3.22	2.58	1.36	3.19	1.89	1.81	1.67	1.98	2.11	1.64	2.36	1.44	0.91	1.63	2.51	1.25	2.37	1.47	1.57	0.96	0.54
V	283	231	296	265	72	67	66	89	66	82	78	92	76	85	84	93	62	8	8	6	6	115	65	138	93	88	125	204
W	1.0	1.0	1.0	1.0	3.0	2.0	2.0	3.0	2.0	3.0	1.0	1.0	1.0	1.0	5.0	2.0	1.0	1.0	1.0	4.0	3.0	2.0	1.0	2.0	1.0	1.0	1.0	1.0
Y	13.5	12.6	13.6	12.5	23.7	23.2	25.4	27.1	26.0	18.5	29.6	26.2	26.5	23.1	23.4	28.1	29.3	18.7	10.4	5.5	10.2	29.7	26.1	34.8	20.3	29.1	16.6	13.2
Yb	1.6	1.5	1.6	1.5	2.3	2.5	2.5	2.8	2.9	2.2	2.9	2.8	2.5	2.3	2.4	2.8	3.0	2.4	1.3	0.4	1.3	3.4	2.2	4.3	1.7	2.9	2.0	1.6
Zn	107	139	81	139	102	90	80	132	94	86	81	83	73	90	82	88	73	17	86	24	97	111	83	76	94	118	97	91
Zr	48	56	82	54	197	180	171	191	168	181	191	210	198	179	182	180	148	44	30	60	31	175	140	139	162	177	65	59

that forms the ME might be complicated. Hence, some authors believe that more investigations are needed to resolve all aspects of the ME genesis (Flinders and Clemens 1995; Chappell 1996). In this study the available data has been used in order to reach the best model for illustrating the genesis of Aligoodarz ME. So, to make a logical conclusion, we first evaluate the most common hypotheses concerning the genesis of ME.

Since there have been many arguments about igneous vs. non-igneous origin of the ME, we first examine if Aligoodarz enclaves are restites or crystallized from a melt. Restite enclaves are mainly enclosed in S-type granitoids, distinctively rich in Al-minerals and show clear metamorphic textures. Textural, mineralogical, and chemical characteristics of restite enclaves indicate that they can indeed result from the melting of crustal rocks. Identification of the restite enclaves in S-type granite is not very difficult. The problem is to apply this model to enclaves in I-type granite with igneous texture. The Aligoodarz ME neither contain andalusite, sillimanite, cordierite, garnet nor residual minerals formed from mica dehydration. On the contrary, igneous textures such as interstitial, poikilitic and osceillatory zoning are features that suggest magmatic crystallization. According to Vernon (1983) and Didier (1984) enclaves with such microstructures are typical magmatic enclaves and do not result from melting processes. Hence, a restite model for the Aligoodarz ME is ruled out.

As mentioned earlier EEG and EET are the two types of igneous ME in the Aligoodarz granitoids. Each type has its own specific set of features and is chemically close to its matching host (Fig. 5). Below, we discuss the typical features of each type and characterize their relations with their hosts.

Enclaves Enclosed in Granodiorite (EEG)

In order to determine what magmatic processes were involved in the formation of the EEG, in this section we evaluate the most common views proposed for the genesis of ME.

Harker diagrams (Fig. 5) indicate that EEG is compositionally intermediate between tonalite and granodiorite but closer to the granodiorite. The intermediary nature of the EEG is better displayed when average composition of tonalite and granodiorite are normalized to the average EEG (Fig. 8). Linear trends in Harker diagrams, and the intermediary position of the EEG indicate that these enclaves are genetically related to granodiorite and tonalite. Such behavior on variation diagrams could generally be interpreted by two fundamentally different models: 1- fractional crystallization. Enclaves with such origin are interpreted as autolithes and are cognate with their host (Donaire et al. 2005; Pascual et al. 2008), and 2- magma

Table 4 Microprobe analyses of biotite, plagioclase and amphibole in ME and their hosts

Biotite	EEG								Granodiorite					EET			Tonalite			
	amphibole-bearing EEG				amphibole-free EEG															
Sample wt%	AL29-240	AL29-249	AL29-251	AL29-256	AL39-170	AL39-173	AL39-175	AL39-176	AL25-106	AL25-108	AL25-109	AL25-111	AL25-112	AL10-81	AL10-86	AL10-87	AL88-63	AL88-65	AL88-77	AL88-78
SiO2	36.74	36.63	36.77	36.68	34.96	35.22	34.88	35.50	34.77	35.64	35.39	35.29	35.16	36.55	36.19	36.22	37.64	37.40	37.51	36.81
TiO2	1.04	2.09	1.66	2.20	3.57	3.05	3.47	1.70	2.28	1.78	1.93	2.00	1.67	4.34	4.05	4.29	1.73	1.83	1.46	1.39
Al2O3	17.52	16.66	17.08	16.52	16.03	16.86	16.80	17.06	17.30	17.07	17.26	17.16	17.30	15.28	15.14	14.86	16.28	16.50	16.72	16.91
FeO	18.02	18.54	18.31	18.88	23.28	22.87	22.51	23.02	22.76	22.40	22.14	22.49	21.68	18.34	19.73	19.42	17.77	17.76	17.90	18.29
MgO	11.01	10.71	11.03	10.74	7.15	7.72	7.27	7.79	7.54	7.93	7.99	7.69	8.05	11.25	10.56	10.71	12.68	12.39	12.45	12.76
CaO	0.12	0.01	0.04	0.01	0.03	0.01	0.53	0.06	0.05	0.03	0.03	0.03	0.11	0.01	0.03	0.01	0.01	0.06	0.03	0.05
Na2O	0.09	0.08	0.09	0.08	0.05	0.07	0.08	0.07	0.07	0.06	0.07	0.03	0.06	0.12	0.13	0.13	0.13	0.11	0.13	0.12
K2O	9.28	9.38	9.16	9.30	9.47	9.57	9.13	9.50	9.50	9.31	8.95	9.61	8.91	9.15	8.67	8.78	8.34	8.27	7.65	7.28
Cr2O3	0.02	0.03	0.06	0.07	0.01	0.06	0.04	0.01	0.04	0.01	0.03	0.03	0.00	0.15	0.16	0.15	0.05	0.06	0.09	0.08
MnO	0.34	0.30	0.32	0.33	0.33	0.33	0.36	0.37	0.41	0.45	0.42	0.44	0.43	0.10	0.06	0.08	0.08	0.09	0.04	0.05
Total	94.18	94.43	94.54	94.81	94.89	95.75	95.07	95.08	94.73	94.68	94.22	94.76	93.36	95.31	94.71	94.64	94.69	94.47	93.99	93.74
Structural formula calculated on the basis of 22 oxygene atoms																				
Si	2.808	2.804	2.803	2.801	2.743	2.728	2.718	2.767	2.724	2.778	2.764	2.757	2.767	2.773	2.776	2.779	2.836	2.825	2.836	2.795
Ti	0.060	0.120	0.095	0.127	0.211	0.178	0.203	0.100	0.134	0.105	0.113	0.117	0.099	0.248	0.233	0.247	0.098	0.104	0.083	0.079
Al	1.578	1.503	1.535	1.486	1.483	1.539	1.543	1.568	1.597	1.568	1.589	1.580	1.605	1.367	1.369	1.344	1.446	1.469	1.490	1.513
Fe	1.152	1.187	1.167	1.206	1.527	1.481	1.467	1.501	1.491	1.460	1.447	1.470	1.427	1.164	1.266	1.246	1.120	1.122	1.132	1.162
Mg	1.254	1.223	1.253	1.222	0.837	0.891	0.845	0.905	0.880	0.921	0.931	0.896	0.944	1.272	1.208	1.225	1.425	1.396	1.403	1.444
Ca	0.010	0.001	0.003	0.001	0.003	0.000	0.045	0.005	0.005	0.002	0.003	0.002	0.009	0.001	0.002	0.001	0.001	0.005	0.003	0.004
Na	0.013	0.011	0.013	0.012	0.008	0.010	0.013	0.010	0.010	0.010	0.010	0.004	0.009	0.018	0.019	0.020	0.019	0.016	0.019	0.017
K	0.905	0.916	0.891	0.905	0.948	0.946	0.908	0.945	0.950	0.926	0.892	0.958	0.894	0.886	0.848	0.859	0.801	0.797	0.738	0.706
Cr	0.001	0.002	0.004	0.004	0.000	0.004	0.002	0.001	0.003	0.001	0.002	0.002	0.000	0.009	0.010	0.009	0.003	0.003	0.006	0.005
Mn	0.022	0.020	0.021	0.022	0.022	0.022	0.024	0.024	0.027	0.030	0.028	0.029	0.028	0.007	0.004	0.005	0.005	0.006	0.002	0.003
Total	7.80	7.79	7.79	7.79	7.78	7.80	7.77	7.83	7.82	7.80	7.78	7.82	7.78	7.74	7.73	7.74	7.75	7.74	7.71	7.73
Mg/(Mg+Fe)	0.521	0.508	0.518	0.503	0.354	0.376	0.365	0.376	0.371	0.387	0.391	0.379	0.398	0.522	0.488	0.496	0.560	0.554	0.553	0.554

Amphibole	EEG				EET				Tonalite			
Sample wt%	AL29-243	AL29-245	AL29-246	AL29-247	AL10-84	AL10-88	AL10-92	AL10-96	AL88-70	AL88-73	AL88-74	AL88-79
SiO_2	54.72	54.15	55.10	53.27	53.48	53.60	53.72	53.70	53.31	53.18	53.08	52.88
TiO_2	0.07	0.11	0.03	0.12	0.19	0.09	0.04	0.04	0.12	0.08	0.18	0.14
Al_2O_3	1.76	2.31	0.89	2.79	0.60	0.70	0.32	0.40	1.81	1.34	2.27	1.91
FeO	13.43	13.31	13.11	14.09	26.57	26.07	26.80	26.56	22.84	23.78	22.43	23.04
MgO	14.82	14.69	15.49	14.18	15.58	15.56	15.19	15.44	16.29	15.69	15.40	15.15
CaO	12.40	12.28	12.16	11.82	0.32	0.49	0.60	0.50	2.17	1.83	3.29	2.77
Na_2O	0.19	0.28	0.14	0.28	0.01	0.04	0.02	0.01	0.16	0.12	0.17	0.13
K_2O	0.03	0.05	0.02	0.04	0.00	0.02	0.00	0.00	0.02	0.02	0.05	0.06
Cr_2O_3	0.03	0.00	0.04	0.02	0.01	0.02	0.00	0.00	0.08	0.06	0.03	0.04
MnO	0.67	0.69	0.77	0.80	0.80	0.81	0.84	0.85	0.60	0.63	0.66	0.69
Total	98.12	97.88	97.73	97.41	97.56	97.40	97.53	97.51	97.40	96.73	97.55	96.81

Structural formula calculated on the basis of 23 oxygene atoms

Si	7.862	7.802	7.934	7.743	7.946	7.961	7.997	7.985	7.836	7.901	7.802	3.754
Ti	0.008	0.012	0.003	0.014	0.021	0.010	0.004	0.004	0.013	0.009	0.020	0.008
Al	0.298	0.392	0.151	0.478	0.105	0.122	0.057	0.071	0.314	0.234	0.393	0.160
Fe	1.613	1.604	1.578	1.712	3.302	3.238	3.337	3.303	2.807	2.954	2.757	1.368
Mg	3.175	3.155	3.325	3.073	3.450	3.446	3.370	3.424	3.569	3.474	3.375	1.603
Ca	1.909	1.896	1.877	1.841	0.051	0.078	0.096	0.080	0.341	0.292	0.518	0.211
Na	0.053	0.077	0.038	0.079	0.002	0.012	0.007	0.003	0.044	0.034	0.048	0.017
K	0.006	0.009	0.003	0.008	0.000	0.003	0.000	0.000	0.004	0.004	0.009	0.006
Cr	0.003	0.000	0.004	0.002	0.002	0.003	0.000	0.000	0.009	0.007	0.004	0.002
Mn	0.081	0.085	0.093	0.098	0.101	0.101	0.106	0.107	0.075	0.079	0.082	0.042
Total	15.01	15.03	15.01	15.05	14.98	14.97	14.97	14.98	15.01	14.99	15.01	7.17

Plagioclase	EEG								Granodiorite				EET					Tonalite					
	amphibole-bearing EEG				amphibole-free EEG																		
Sample wt%	AL29-225	AL29-231	AL29-232	AL29-237	AL39-115	AL39-159	AL39-160	AL39-122	AL25-89	AL25-93	AL25-100	AL25-105	AL10-109	AL10-100	AL10-101	AL10-102	AL10-103	AL88-82	AL88-83	AL88-84	AL88-85	AL88-86	AL88-87
SiO_2	56.23	55.13	50.92	48.38	60.70	54.68	49.68	57.95	58.51	56.97	54.27	60.11	55.22	56.45	54.25	45.23	55.44	56.46	55.86	46.56	47.56	45.37	46.20
TiO_2	0.05	0.00	0.01	0.00	0.02	0.01	0.03	0.02	0.01	0.00	0.00	0.00	0.01	0.01	0.00	0.00	0.02	0.00	0.00	0.00	0.02	0.04	0.00
Al_2O_3	27.98	28.61	31.40	33.28	25.24	28.22	31.96	26.57	26.36	27.15	28.78	25.30	27.87	26.97	28.50	34.34	27.58	27.85	28.15	34.22	33.73	34.92	34.46
CaO	10.34	11.07	14.25	16.65	6.65	10.79	14.99	8.57	8.13	9.08	11.34	6.93	10.39	9.35	11.17	18.07	10.09	10.08	10.51	17.92	17.10	18.70	18.15
Na_2O	5.82	5.46	3.43	2.31	7.79	5.56	3.26	6.81	6.97	6.44	5.21	7.02	5.90	6.36	5.44	1.30	5.97	6.11	5.71	1.63	1.99	1.10	1.46
K_2O	0.06	0.07	0.04	0.03	0.12	0.07	0.03	0.17	0.16	0.15	0.09	0.09	0.04	0.04	0.03	0.01	0.05	0.03	0.03	0.00	0.02	0.01	0.01
Total	100.52	100.38	100.09	100.68	100.54	99.40	100.05	100.14	100.15	99.84	99.74	99.46	99.49	99.23	99.46	98.99	99.24	100.68	100.34	100.38	100.44	100.15	100.31
Structural formula calculated on the basis of 8 oxygene atoms																							
Si	2.516	2.48	2.314	2.203	2.685	2.481	2.268	2.592	2.612	2.560	2.457	0.00	2.501	2.554	2.463	2.106	2.515	2.523	2.505	2.135	2.173	2.090	2.121
Ti	0.002	0.00	0.000	0.000	0.001	0.000	0.001	0.001	0.000	0.000	0.000	2.683	0.000	0.000	0.000	0.000	0.001	0.000	0.000	0.000	0.001	0.001	0.000
Al	1.475	1.51	1.682	1.786	1.316	1.509	1.720	1.401	1.387	1.438	1.535	0.000	1.488	1.438	1.525	1.884	1.474	1.467	1.488	1.850	1.817	1.896	1.865
Ca	0.496	0.53	0.694	0.812	0.315	0.525	0.733	0.411	0.389	0.437	0.550	0.000	0.504	0.453	0.543	0.901	0.491	0.483	0.505	0.880	0.837	0.923	0.893
Na	0.505	0.48	0.303	0.204	0.668	0.489	0.289	0.591	0.603	0.561	0.457	0.331	0.518	0.558	0.479	0.117	0.525	0.529	0.496	0.145	0.177	0.098	0.130
K	0.004	0.00	0.002	0.002	0.007	0.004	0.002	0.010	0.009	0.009	0.005	0.607	0.003	0.003	0.002	0.001	0.003	0.002	0.002	0.000	0.001	0.000	0.000
Total	5.00	5.00	5.00	5.01	4.99	5.01	5.01	5.00	5.00	5.00	5.00	3.62	5.01	5.01	5.01	5.01	5.01	5.00	5.00	5.01	5.01	5.01	5.01
An	49.4	52.64	69.5	79.8	31.8	51.6	71.6	40.6	38.8	43.4	54.3	35.1	49.2	44.7	53.1	88.4	48.1	47.6	50.4	85.8	82.5	90.3	87.2
Ab	50.3	46.99	30.3	20.0	67.5	48.1	28.2	58.4	60.2	55.7	45.1	64.3	50.5	55.0	46.8	11.5	51.6	52.2	49.5	14.1	17.4	9.6	12.7
Or	0.4	0.38	0.2	0.2	0.7	0.4	0.2	0.9	0.9	0.8	0.5	0.6	0.2	0.3	0.2	0.1	0.3	0.2	0.2	0.0	0.1	0.0	0.0

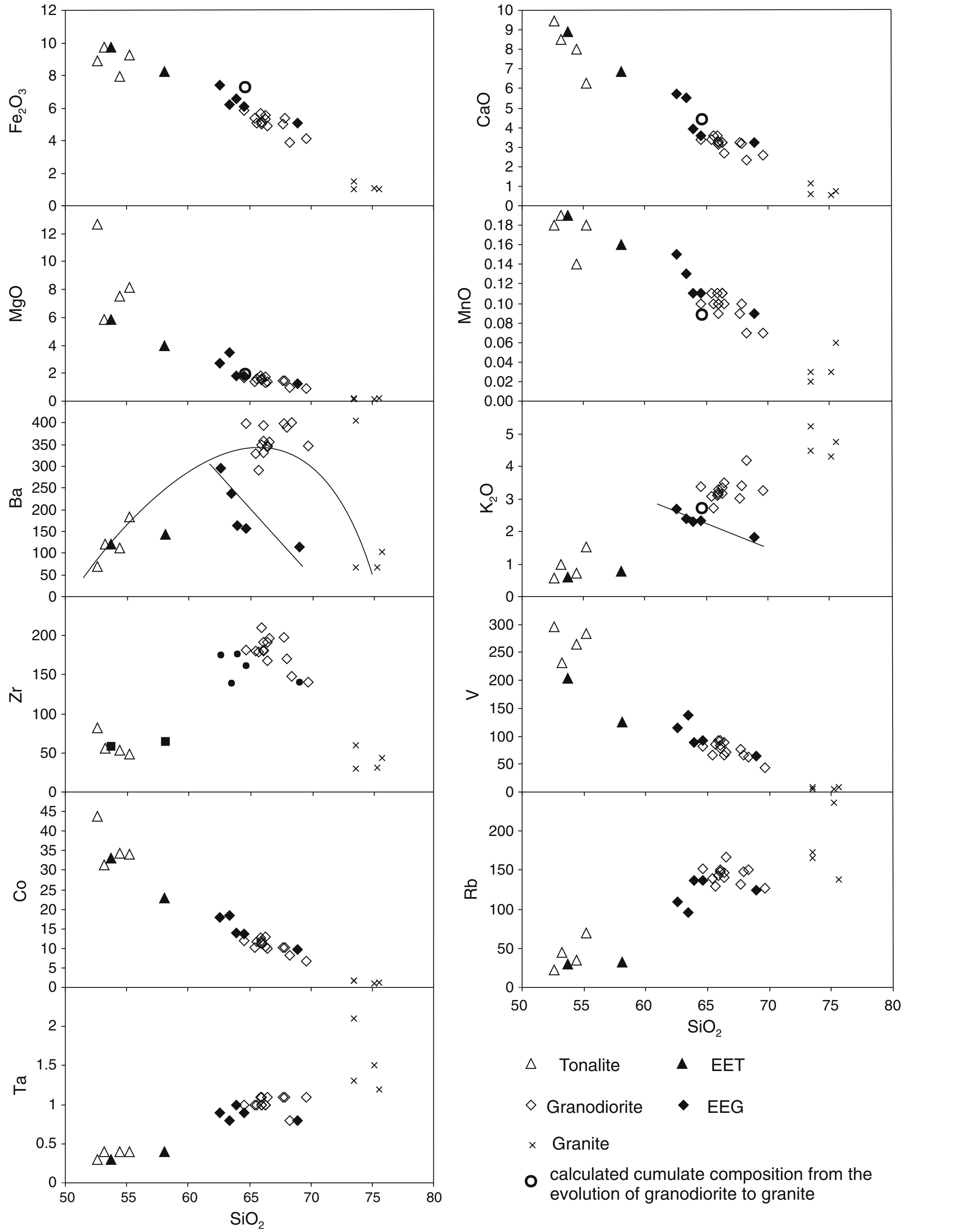

Fig. 5 Plots of some major and trace elements versus SiO_2. The EEG show different trends from the remaining samples in plots of silica against K_2O and Ba. Calculated composition of extracted cumulates after 69% crystallization of the parent granodiorite is shown as a circle on major oxide plots

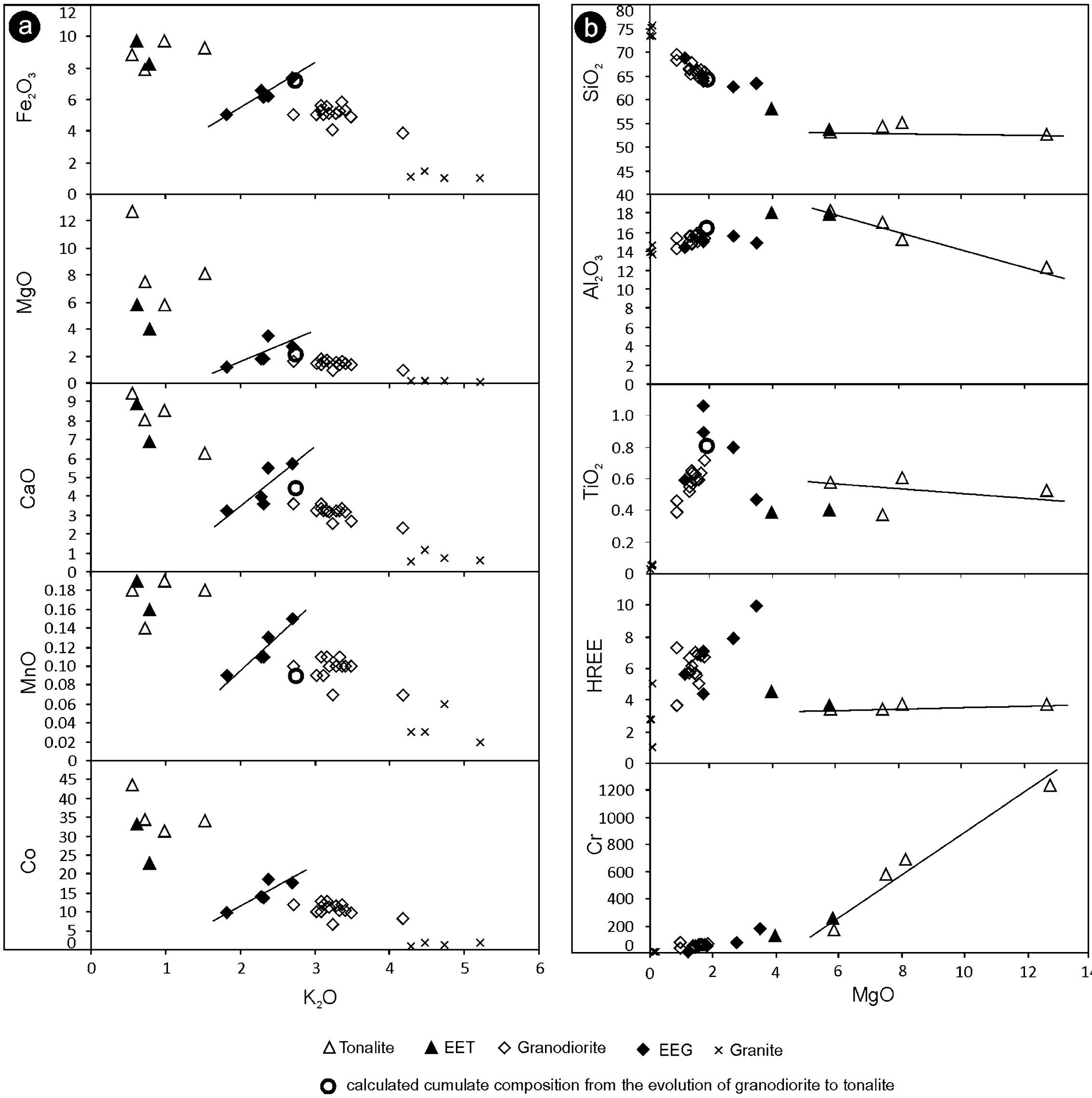

Fig. 6 Major and trace elements vs. K_2O (**a**) and MgO (**b**) variation diagrams. Calculated composition of extracted cumulates after 69% crystallization of the parent granodiorite is shown as a circle on major oxide plots. When K_2O is considered as the variation index, the trends for EEG are different from the rest. By increasing K_2O, the enclaves become more enriched in compatible elements. Ba demonstrates the same behavior but not shown here. When MgO is considered as the fractionation index, variation trends of tonalites are different from the remaining samples and composition of EEG is closer to that of their host granodiorite

mixing. In this model isolated fragments of more mafic (enclave) magma are enclosed in a second felsic (host) magma and subsequently, chemical and mineral exchange between the enclaves and their host drives the chemical composition of the enclaves closer to that of the host. (Dorais et al. 1990; Allen 1991; Barbarin and Didier 1991; Blundy and Sparks 1992; Tepper and Kuehner 2003).

In the following sections we discuss both magma mixing and fractional crystallization as the potential processes that formed the EEG.

Evidence against the role of magma mixing in forming the EEG

Several properties of the EEG and their relation with the enclosing host rocks discount the possibility of involvement of magma mixing. This argument is based on field, microscopic and chemical observations and backed up by mixing test discussed below.

Field evidence In the well-known examples of mixing of mafic and felsic magmas suggested for the origin of ME, as

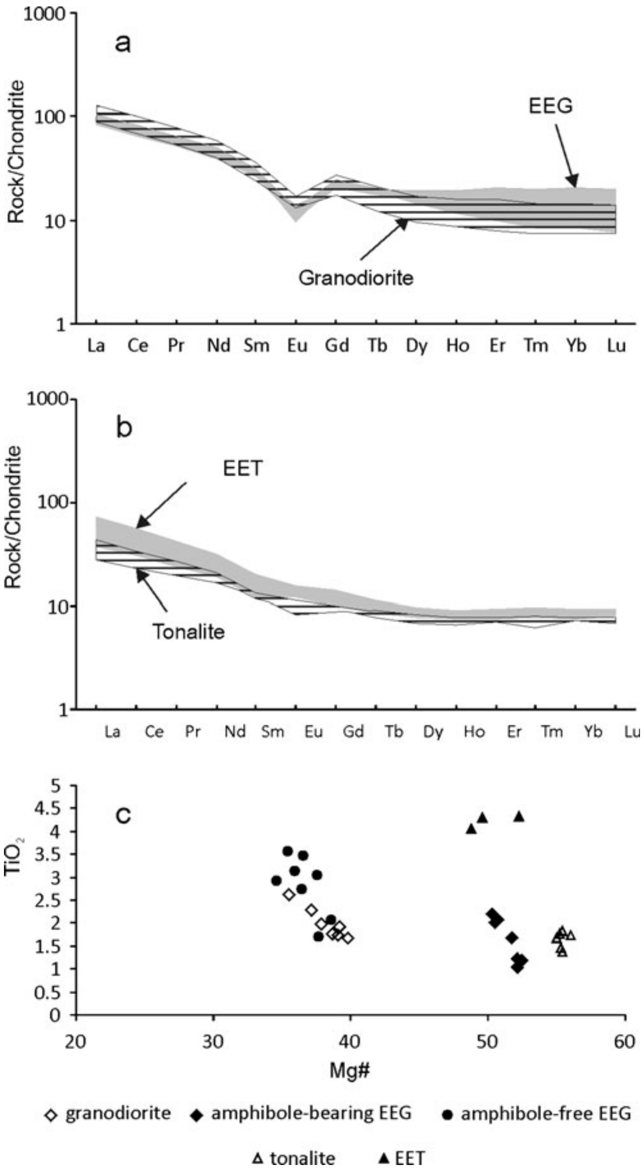

Fig. 7 Chondrite normalized (Boynton 1984) REE patterns of: **a**) EEG and their host granodiorite; **b**) EET and their host tonalite. HREE enrichment in some EEG corresponds to those enclaves containing amphibole. **c**) TiO_2 vs. Mg# diagram for biotites in the EEG, EET and their hosts. Biotites of amphibole-free EEG and their host granodiorite cluster together and form a coherent trend which implies crystallization from the same melt. However, in terms of Mg#, biotites of amphibole-bearing EEG are very different from those of amphibole-free EEG and the host granodiorite, probably suggesting a time lag in crystallization and enclave formation sequence. Biotites in the EET and their host tonalite are hugely separated in relation to TiO_2, indicating formation from different magmas. Chemical proximity of biotites of amphibole-bearing EEG to those of the tonalites could be interpreted in terms of sub-tonalitic nature of the magma from which the granodiorites were evolved (see stage "1" in Fig. 10a)

enclave population increases, the host composition shifts towards the enclave composition (e.g. Silva et al. 2000). Such relation is not observed in Aligoodarz granitoids; although the EEG is more abundant in Mollataleb than in Khorheh, composition of the host granodiorite is generally the same in the two locations (Fig. 1). This chemical homogeneity suggests that mixing or mingling has not played a major part in formation of the EEG.

Chemical exchange effectively occurs when both the mafic and the felsic end-members are partly liquid (e.g. Wiebe 1973). The EEG has sharp boundaries and lack concentric zoning within and around the enclaves indicating that chemical interactions with the host granodiorite were far from mixing. Also, chilled margin is expected to occur in enclaves resulted from mixing of two magmas with contrasted temperature (e.g. Wiebe et al. 1997). The Aligoodarz enclaves lack chilled margins suggesting small temperature difference between enclave and host magma (Troll et al. 2004; Chen et al. 2009) or participation of enclaves as solid materials in the host magma (Donaire et al. 2005). Furthermore, injection of host magma into enclaves (Fig. 3b) indicates that at least some enclaves had entered the host in relatively solid state. In such enclaves, absence of gradational contacts between enclave and injected magma indicates high rheology contrast. Local magma mingling/mixing between enclaves and the host might have occurred but only in limited scale. Angular form of some enclaves (Fig. 3a) confirms this interpretation. In summary, field observations attest that enclaves were initially solid/near solid, rule out possibility of magma mixing.

Microscopic and chemical evidence Both in the enclaves and their host the highest anorthite contents correspond to the cores of plagioclases. The highest An content in plagioclase phenocrysts in the EEG is An_{80} whereas, in the host granodiorite the cores are up to An_{55}. Plagioclase phenocrysts show complex patchy and oscillatory zoning and consist of irregular resorbed zones (Fig. 4b). Resorption textures can be caused by either magma mixing (e.g. Wiebe 1968; Vernon 1991; Chen et al. 2009), or decompression (Alfred and Anderson 1984; Nelson and Montana 1992; Singer 1993). In case of magma mixing, more calcic plagioclase fills or overgrowths the resorption zones; whereas in decompression, plagioclase with similar or even lower An% forms in and around the resorbed cores as observed in the EEG.

Although introduction of crystals from host magma into enclave magma has been documented (e.g. Feeley and Dungan 1996), distribution of zircon in the EEG, granodiorite and tonalites seems to be particularly meaningful in evaluating magma mixing possibly because many zircons are included in biotites, and so, basically shielded from chemical exchange between supposed two melts (Bea 1996). Also zircons which are not included in biotites have relatively different sizes from those in the host. Zr concentration (a measure of modal abundance of zircon)

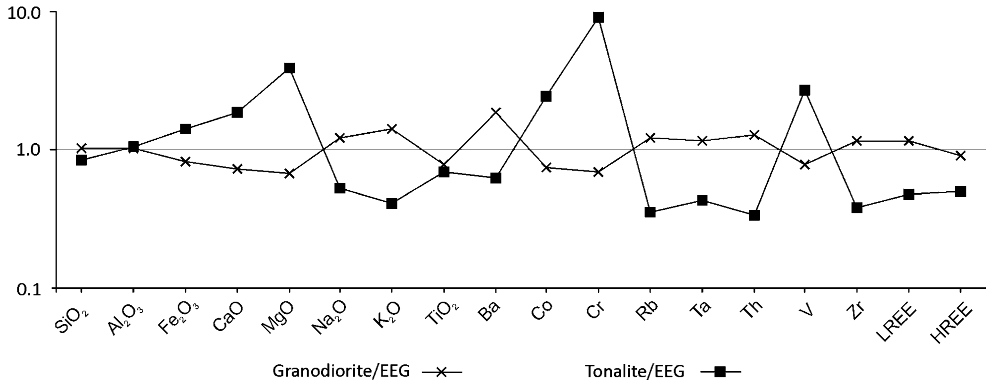

Fig. 8 Average chemical composition of granodiorite and tonalite normalized to the average composition of EEG. For most elements, EEG has chemical composition intermediate of tonalite and granodiorite but TiO_2 and HREE are more enriched in EEG

in the EEG and the host granodiorite is about the same and is higher than the tonalite. This distribution pattern is more consistent with the EGG being resulted from a parent melt more similar to the host granodioritic magma than an intermediate melt which is theoretically less enriched in Zr.

Occurrence of amphibole in a subset of the EEG and its absence in the host granodiorite seems to be useful in constraining the degree of chemical exchange because a contrast in mineralogy of the enclave-host pair indicates that full equilibration has been prevented either by access or by thermodynamic considerations (Stephens et al. 1991). This particularly applies to the EEG and their host because there are enclaves with similar size but different chemistry and contrasting mineralogy within a single outcrop of the homogeneous granodioritic host.

Among EEG samples, two from the amphibole-bearing type are more enriched in HREE (Fig. 6b). HREE-enrichment of the EEG is also noticeable in Figs. 7a and 8. REE are generally considered as the trace elements least likely to equilibrate (Holden et al. 1991). It has also been emphasized that equilibration rates for HREE are lower than LREE (Kumar and Rino 2006). Therefore, HREE-enrichment observed in some EEG cannot be caused by chemical modification. Similarly, some of the EEG are also enriched in TiO_2 (Figs. 6b and 8). Magma mixing model is unlikely because mafic rocks with higher HREE and TiO_2 are absent in the region. Such HREE and TiO_2 enrichments could just be due to amphibole and possibly Fe-Ti-oxides accumulation.

Igneous biotite continuously equilibrates with its host liquids (Barbarin 2005). So, the composition of biotites in the enclaves should be similar to those in the host if magma mixing takes place. Differences in biotite composition of the amphibole-bearing EEG and the biotites of the host exclude occurrence of extensive equilibration which is common in enclaves generated by magma mixing.

The EEG shows different trends relative to the trends of other samples in plots of incompatible elements (K and Ba) vs. SiO_2 (Fig. 5) or compatible elements vs. K_2O (Fig. 6a). Ba behavior is similar to K_2O but it is not shown. The positive correlation between K_2O, Ba and compatible elements is not easy to explain in terms of magma mixing because a high Ba and K mafic end member is uncommon in plutonic arcs and nonexistent in the region. Moreover, in spite of the host granodiorite contain relatively constant levels of Ba and K_2O, concentrations of those elements in the EEG are quite variable (Fig. 5). Such behavior of Ba and K_2O indicates that continuous enclave-host diffusion and equilibration for Large Ion Lithophile Elements (LILE), which is so common and permitted in magma mixing (e.g. Holden et al. 1991), did not take place for the EEG. Instead, such observation is consistent with enclave generation by biotite accumulation (Donaire et al. 2005; Pascual et al. 2008) because biotite has high partition coefficient for K and Ba and the falling K and Ba content in amphibole-free EEG is due to lower abundance of biotite (Table 1). Similarly, K-feldspar is the main host for these elements but due to low K-feldspar contents, variable K and Ba concentrations must be controlled by different abundance of accumulated biotite.

To conclude, we apply the mixing test of Fourcade and Allègre (1981) for investigating whether the EEG are indeed hybrid rocks resulted from mixing of felsic granodioritic and intermediate tonalitic magmas. For this test we consider the most mafic enclave with the lowest SiO_2 content (sample AL12-1) to be representing the hybrid magma, and average compositions of the granodiorite and the tonalite are considered as the initial felsic and intermediate end members, respectively. The following equation can be applied for each element (Fourcade and Allègre 1981):

$$\left(C_M^i - C_A^i\right) = X\left(C_B^i - C_A^i\right)$$

where

C_M^i content of i element in hybrid magma
C_A^i content of i element in felsic magma
C_B^i content of i element in intermediate magma, and
X the mass fraction of the component B

Calculated concentrations of major and selected trace elements are plotted on $\left(C_M^i - C_A^i\right)$ vs. $\left(C_B^i - C_A^i\right)$ diagram (Fig. 9a). Slope of the straight line through the major

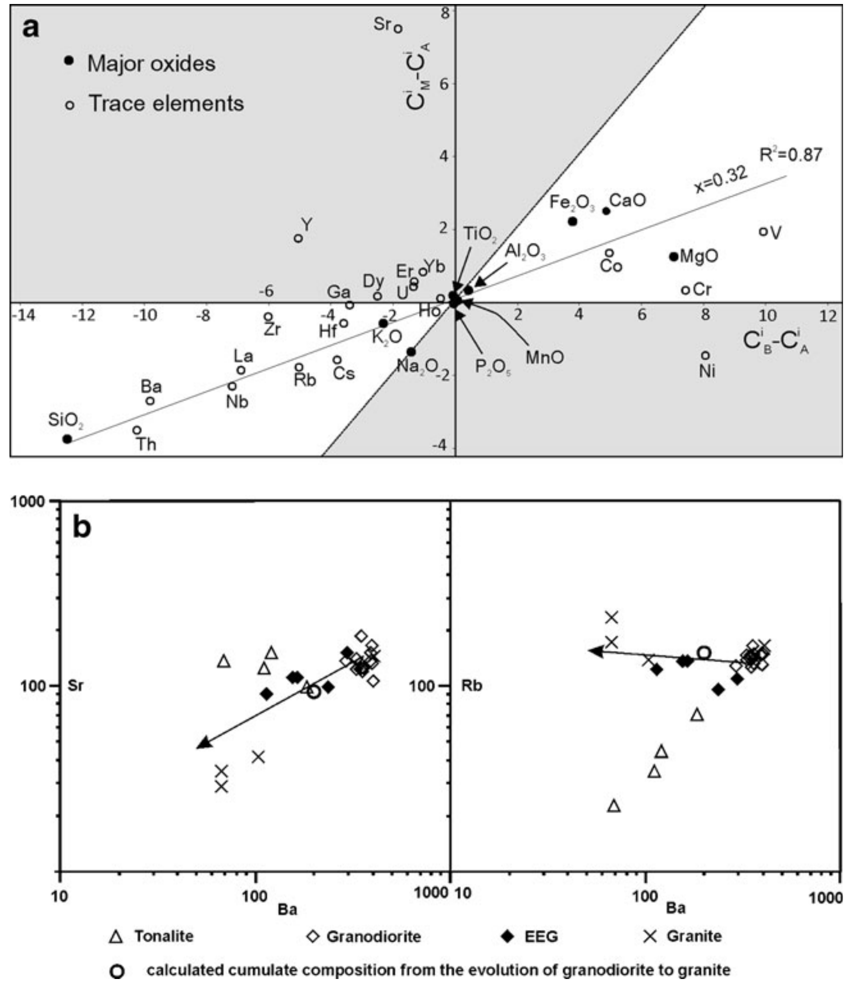

Fig. 9 **a**) Mixing test between granodioritic and tonalitic magmas for production of the hybrid enclave AL12-1. The shaded areas correspond to the domains where the mixing model is not verified. C_M^i= concentration of element i in hybrid magma (enclave); C_A^i= concentration of element i in felsic component (granodiorite); C_B^i= concentration of element i in intermediate component (tonalite); R^2 = correlation coefficient on the basis of plots of major oxides; and x = fraction of intermediate component in enclave magma based upon the straight line drawn for major oxides. $\left(C_M^i - C_A^i\right)$ and $\left(C_B^i - C_A^i\right)$ for some trace elements were too high and to fit them in the range of X and Y axes each was multiplied by a factor <1. **b**) Plots of Sr and Rb vs. Ba. Fractional crystallization vectors correspond to 69% Rayleigh fractionation. Cumulate assemblage composed of 32% quartz, 42% plagioclase and 26% biotite. Partition coefficients are from Arth (1976); Nash and Crecraft (1985). Average composition of granodiorite considered as the starting point

elements oxides gives the mass proportions of the mixture. The slope of 0.32 means that participation of 32% of the tonalitic end member could produce the enclave sample AL12-1. However, major oxides TiO_2 and Na_2O and trace elements Sr, Y, Dy, Er, U, Yb, Ho and Ni plot in the shaded parts which correspond to mixing forbidden domains, suggesting that binary magma mixing cannot explain the abundance of these elements in the EEG (Fourcade and Allègre 1981). Magma mixing is not adequate in explaining genesis of the EEG also because for producing enclave AL12-1 with 32% of the initial intermediate magma, extensive chemical exchange with granodioritc melt is required which is not confirmed by observations.

Evidence for cognate nature of the EEG

The evolutionary trends shown in Fig. 5 support fractional crystallization. Fe_2O_3, CaO, MgO and V decrease with increasing SiO_2. These negative trends are consistent with fractional crystallization of biotite, amphibole, plagioclase and Fe-Ti oxides. Also, increasing incompatible K_2O and Rb with increasing SiO_2 is consistent with late stage fractionation of K-feldspar. An example of chemical variation caused by fractional crystallization is that for Ba and Zr (Chappell 1996). As seen in Fig. 5, Ba and Zr concentration drops rapidly after biotite and zircon appear as a crystallizing phase in granodiorite. General increase in REE from tonalite to granodiorite reflected the influence of fractional crystallization (Fig. 7a–b). Concave-upward and partial differentiation of LREE from HREE in REE patterns of residual melts have collectively been suggested to be controlled by amphibole fractionation (Gromet and Silver 1987; Sawka and Chappell 1988; Romick et al. 1992; Blundy and Wood 2003). The decrease in Eu/Eu* from tonalite to granodiorite, probably correlates with progressive removal of plagioclase from the magma. Moreover, our radiogenic isotopic studies on Aligoodarz granitoids reveal that tonalites and granodiorites are cogenetic and originated from crustal source. Thus it seems that the EEG, being genetically linked to granodiorite and tonalite, is the result of the same evolutionary process. In Table 5 some differences in features of enclaves resulted from magma mixing and EEG are summarized. In the following

Table 5 Comparison of some features between enclaves resulted from magma mixing with the EEG

Features	Enclaves resulted from magma mixing (Didier and Barbarin 1991 and many other references cited in the text)	EEG
Relationship between abundance of enclaves and composition of the host	Observed	Not observed
Occurrence of chilled margin	Observed	Not observed
Similarity between chemical composition of biotite in enclaves and host	Observed	Not observed
Similarity in mineral paragenesis of enclaves and the host	Observed	Not observed
Records of mixing in plagioclase grains	Observed	Not observed
Compatibility in concentration of elements in enclaves in comparison with mafic and felsic end member magmas	Observed	Not observed (e.g. HREE, TiO_2, K_2O, Ba and Zr)
Earlier physical state of the enclaves before entering the host	Molten	Solid

we discuss two potential processes that correspond to fractional crystallization and could account for the origin of EEG.

A) EEG as cumulate enclaves

Some enclaves in granitoids have been interpreted to be cumualtes (Bébien 1991; Platevoet and Bonin 1991). In applying this hypothesis to the Aligoodarz enclaves, the EEG would be seen as the disrupted fragments of cumulate tonalitic assemblages later disrupted and dispersed in the granodioritic magma. Such scenario fails for the following reasons:

Cumulate enclaves are distinct from the regular microgranular enclaves in being consisted of crystals as large as those in their hosts and showing cumulate textures (Barbarin 1991; Bébien 1991; Didier and Barbarin 1991, p. 23). In many granitoids such as the Sierra Nevada batholith, cumulate enclaves appear together with regular ME. Lack of recrystallization textures in the ME precludes formation after coarse-grained cumulate enclaves (Barbarin 1991, 2005). In such cases each enclave type has originated by different processes.

In Section "Granodiorite and their enclaves" a group of closely spaced, coarse-grained xenolithic enclaves was introduced. They are disrupted fragments of tonalites and are restricted to the tonalite-granodiorite border (Fig. 3c). By considering the same origin for the EEG, it is difficult to explain their chemical behavior because they are more similar to their hosts in comparison with their hypothetical tonalitic source (Fig. 6b). Also tonalites show different trends from other samples suggesting earlier crystallization from less evolved magma and accumulation of more primitive minerals (e.g. Wilson 1989). Such chemical differences between tonalites and EEG combined with lack of recrystallization makes the cumulate enclaves distinct from the EEG and advocate a non-cumulate origin for the latter.

B) EEG as disrupted fragments of rapidly cooled fine-grained borders (chilled margins)

Crystallization in borders of the magma chamber or its feeding conduits, where temperature gradient is steeper, is the mechanism that we advocate as the origin of the EEG based on observations described in the following.

Where the enclaves are uniform in terms of grain-size and display simple curved or straight boundaries with no chilled margins, they might have come into contact with the host granodiorite in completely solid form (Wiebe et al. 1997). This is consistent with rapid cooling in areas of the melt system and is supported by occurrence of acicular apatite in the EEG, also experimentally shown to be indicating rapid cooling (Wyllie et al. 1962).

The least siliceous EEG shows the highest K_2O and Ba (Fig. 5). K_2O- and Ba-rich enclaves also contain higher Fe_2O_3, MgO, MnO and compatible trace elements such as Co (Fig. 6a) and indicate biotite precipitation. Biotite accumulation in enclaves could result from rapid cooling under which the mafic minerals crystallize with more rapid nucleation rate than the tectosilicates (Naney and Swanson 1980). This process also explains presence of amphibole and relative scarcity of K-feldspar in the EEG.

The amphibole-bearing EEG might have formed earlier than the amphibole-free ones when the magma was less evolved. Differences between amphibole-bearing and amphibole-free EEG in terms of intensity and profusion of the patchy zoning in plagioclases confirm this interpretation, as in the former patchy zoning is more common suggesting their origination at deeper levels followed by larger decompression (Fig. 4b). The time lag in crystallization of amphibole-bearing and amphibole-free EEG could also be inferred from the vastly different Mg# of their biotites with the former plotting near the least evolved and the latter clustering among the more evolved granodiorites (Fig. 7c), presupposing that all EEG were derived from the same original magma.

Geochemical modeling of the EEG

For supporting our cognate model both mass balance and trace element modeling were performed. PETROGRAPH program (Petrelli et al. 2005) was used for mass balance calculation to produce enclaves chemically similar to the EEG by fractional crystallization assuming that 1) granodiorite is the parent magma from which the more evolved granite is derived, and 2) the type and composition of fractionated minerals are similar to those of the amphibole-free EEG (Table 4). The modeling shows that by 69% crystallization of a mineral assemblage composed of 32% quartz, 42% plagioclase and 26% biotite from the original magma an evolved melt similar to average granite can be produced. This percentage of crystal fractionation may seem too large for granitic systems but is compatible with scarcity of granites in the study area. As the results show, the calculated cumulate assemblage is modally similar to the amphibole-free EEG (Table 1). Harker diagrams (Figs. 5 and 6) also show that the calculated cumulate is chemically similar to the actual EEG in terms of major oxides.

Trace element modeling based on results from the mass balance calculation and by using Rayleigh fractionation also yielded trace elements contents that roughly match with the amphibole-free EEG. The result is presented in Table 6. C_R is calculated cumulate composition, C_0 correspond to average composition of granodiorite and D is the bulk partition coefficient. Accumulated assemblage composed of 32% quartz, 42% plagioclase and 26% biotite. 69% Rayleigh fractionation is assumed. Partition coefficients are from Arth (1976); Pearce and Norry (1979); Nash and Crecraft (1985). In Fig. 9b, our samples are plotted on Sr and Rb vs. Ba and are compared with composition of the calculated cumulate. Excel spreadsheet of Keskin (2002) was used to show the compositional shift of the evolved melt after 69% fractionation of the parent magma. As it is shown, extraction of such cumulate assemblage shifts the composition of derived melt toward the granite.

Table 6 Average composition of amphibole-free EEG that is compared with calculated cumulate composition derived from initial granodioritic magma

element	D	C_0	C_R	Amphibole-Free EEG
Rb	0.9	145.7	153.2	132.5
Sr	2.0	132.7	92.4	104.5
Ba	2.7	360.7	194.0	144.2
cs	0.8	8.4	8.9	6.0
Hf	0.3	5.3	7.0	4.5
Nb	1.7	13.0	10.1	12.8
Ta	0.4	1.0	1.3	0.9
Th	0.3	13.9	18.1	11.0
U	0.2	2.1	2.7	1.4
Y	0.4	25.4	32.1	25.2
La	1.7	34.8	27.3	29.9
Ce	1.3	71.1	64.7	61.5
Nd	0.8	30.7	33.6	27.9
Sm	0.6	6.3	7.4	6.0
Eu	1.5	1.1	0.9	0.9
Tb	0.5	0.9	1.1	0.9
Dy	0.5	4.9	6.0	5.2
Yb	0.4	2.6	3.2	2.3
Lu	0.4	0.4	0.5	0.3
Cr	5.1	51.5	11.1	36.7

We were not able to produce the evolutionary trend from granodiorite to granite by extracting the amphibole-bearing EEG. One possible explanation could be that after enclave formation the remaining liquid underwent further fractional crystallization not recorded in the enclave assemblage. Alternatively, the parent magma for this type of ME could have been somewhat dissimilar to the existing granodiorite host, i.e., these enclaves were probably derived from a relatively less evolved parent not present at this level of exposure. Extraction of amphibole-bearing enclaves from such magma might have shifted the composition of the evolved magma toward the granodiorite, as implied in Fig. 10a.

Figure 10a attempts to show the evolutionary scenario for formation of the EEG along rapidly-cooled zones in a magma chamber as conceived from the above-mentioned discussion and modeling. We suggest that the amphibole-bearing EEG crystallized before the crystallization of amphibole-free enclaves. It is noteworthy that rapidly-cooled margins do not exclusively appear in the magma chambers and could form along the feeding conduits as well.

If the chilled margins were thick enough, then the enclave rheology, correlating with crystal/melt ratio, would considerably vary across the chilled margin and the degree

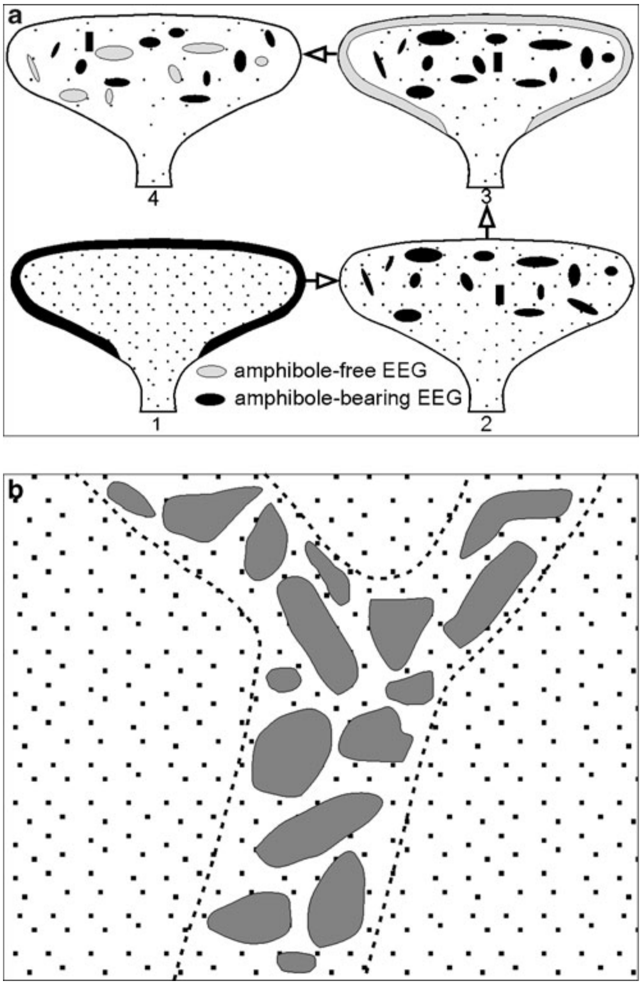

Fig. 10 **a**) Chilled margin model (e.g., Donaire et al. 2005) for illustrating development of the EEG. 1) Formation of rapidly-cooled borders (*chilled margins*) during earlier stage of the magma evolution, characterized by crystallization of biotite + amphibole as the mafic components, 2) Forceful ascend of magma and disruption of chilled margins to produce amphibole-bearing EEG dispersed in the remaining magma, 3) Formation of new and amphibole-free chilled margin with a more evolved composition, 4) Ascending of magma and disruption of new chilled margins. As a result, two types of enclaves with different mineralogy occur in the granodiorite. Chilled margins may also develop on conduit walls not shown in this figure. Variation in density of the dots corresponds to compositional changes of the host magma. **b**) Model for explaining the origin of the EET by the injection of a more mafic magma (*gray*) into the highly crystallized tonalitic host (*stippled*) and the subsequent break-up into a composite dike shown as inclusion trains of the injected magma due to interaction with the host (After Barbarin and Didier 1992; Barbarin 2005)

of local mingling/mixing (Fig. 3b) might therefore vary from enclave to enclave. In addition to rheology variation, magnitude of post-fragmentation movement in the host magma could have influenced the final shape of the enclaves; i.e., higher plasticity along with greater spinning within the host magma could have reduced angularity of the enclaves originating from the less rigid parts of the chilled margin.

Relationship of granites to granodiorites by a process of fractional crystallization -as shown above- may require enclosing of some enclaves in the end product. Absence of enclaves in the granite could be the result of their gravitational segregation over relatively long residence followed by effective separation of the granitic melt by filter pressing. It is worth noting that the granite cross-cuts the granodiorite as dikes.

Overall, it seems that the EEG corresponds to the relatively solid fragments present in the granitoids at the time when magmatic flow prevailed. Mechanical interactions caused crushing of the rapidly cooled margins and scattering of the resulted fragments inside the dynamic magma chamber and the feeding conduits. Enclaves of this kind are typical of plutons emplaced in the upper crust where large temperature contrast between injected magmas and the host country rocks exists and results in formation of microgranular textures (Barbarin and Didier 1991).

Enclaves Enclosed in Tonalite (EET)

Table 2 summarizes the major differences between the EET and the EEG. Plagioclase is an important phase in preserving information about the enclave forming processes (e.g. Chen et al. 2009) and microprobe results for plagioclases in the tonalites and their enclaves were presented in Section "Tonalite and their enclaves". Plagioclase phenocrysts showing patchy zoning occur in both the EET (Fig. 4f) and the host but generally close to the contact with the enclaves (Fig. 4d). It seems that the plagioclase phenocrysts occurring in the EET are actually those crystallized in the host and subsequently migrated into the enclaves. Both types are rimmed by more sodic plagioclase (Fig. 4e–f). The substantial chemical difference between the rim and the spongy core suggests a significant change in environment prior to rim crystallization. Similar observations have been made elsewhere in the world and were experimentally investigated (e.g. Nelson and Montana 1992). Enclaves with such textures and such kind of relation with the host can be accounted for as composite (fragmented) dikes injected into a largely crystallized host (Barbarin and Didier 1992; Barbarin 2005). Occurrence of such enclaves as clusters in few locations supports the dependence of enclave formation with dikes intrusion. We find this model largely applicable to the plagioclase phenocrysts in the EET and their tonalitic host (Fig. 10b). Generally speaking, disequilibrium induced by injection of a different magma is expected to cause partial resorption of the plagiocalses in the contact zone, and in reference to the EET, by moving away from the enclave, the number of such plagioclases and the intensity of resorption decrease in the tonalite host; an observation which lends more support to Barbarin and Didier (1992) and Barbarin (2005) model (Fig. 10b).

Interfingering of new magma with largely crystallized tonalitic host and consequent physiochemical interaction between the two make EET distinct from EEG. Such interactions were aided by a combination of factors such as: 1- local temperature rise and viscosity fall due to the injection of the hotter new magma (Fig. 10b), 2- reduction of melting point resulted from volatile migration from the injected magma into the semi-liquid host and further reduction of its viscosity (Castro et al. 1990, 1991), and 3- enhancing convection in the region adjacent to the newly injected magma (Furman and Spera 1985). The rate of chemical interaction depends on the chemical contrast between enclaves and the host and on melt/crystal ratio. Mineralogical differences between the EET and the host rock suggest that limited chemical interaction has occurred. Yet, evidence of interactions includes pyroxenes rimmed by new amphibole and late plagioclase with same anorthite content in both enclave and the host that crystallized after interaction and enveloped the more calcic plagioclase cores (Fig. 4e-f). Such low-Ca plagioclase also fills the resorbed hollows in the interior parts of the phenocrysts (Fig. 4e–f). Probably interaction between late stage SiO_2-enriched interstitial liquids of the host with the injected magma shifted the enclave composition toward higher SiO_2 levels (Fig. 5).

Conclusions

Petrographic data combined with whole-rock and mineral chemistry were presented in this paper to introduce two different types of microgranular enclaves (ME) in the Aligoodarz calc-alkaline granitoids of western Iran and investigate their origins. Enclaves enclosed in granodiorite (EEG), although relatively more mafic, are chemically very similar to their host. Commingling of magmas of different composition does not explain formation of the EEG as our observations disqualify large chemical equilibration with the host and rather suggest a cognate origin by rapid cooling at the margins of the magma chamber or conduit walls under which crystallization of biotite ± Fe-Ti-oxides ± amphibole prevailed.

Enclaves enclosed in tonalite (EET) show relatively sharp, intertwined boundaries and similar chemistry to their host. They are inferred to be small magmatic pulses that intruded the early fractures of a nearly-solid tonalitic body and were transformed into inclusion trains. Differences in physical state of the injected magma from its corresponding host prevented comprehensive mixing, however, grain transfer from the host rock into the enclave and interaction of the enclave magma with late stage fluids from the host tonalite imply some degrees of mixing and mingling.

Patchy zoning is common in plagioclases of the Aligoodarz enclaves. However, mechanisms causing such textures are different in each group of enclaves. In case of the EEG, patchy zoning is explained by instability-induced resorption resulted from decompression, but the resorption texture in the EET plagioclases was presumably caused by interaction with a new magma.

Aligoodarz granitoids provide an opportunity for demonstrating how rapid cooling on the margins of a shallow magma chamber and the conduit walls in the roots of a continental arc produces enclaves as the result of fractional crystallization with disturbed order. Generation of such enclaves can have an important role in the evolution of mafic granitoid magmas. In this case study magma mixing seems to have been limited and broad chemical equilibration with the host might not have occurred.

Acknowledgments Constructive criticisms from Teodosio Donaire, Finger Fritz and Georg Hoinkes have helped to improve the manuscript. Riccardo Vannucci from University of Pavia, Italy is also acknowledged for his helps. Support for this work was provided by the Iran National Science Foundation (INSF), Grant no. 87020210, and Tectonics Observatory of California Institute of Technology, USA.

References

Ahmadi Khalaji AA, Esmaeily D, Valizadeh MV, Rahimpour-Bonab H (2007) Petrology and geochemistry of the granitoid complex of Boroujerd, Sanandaj-Sirjan Zone, Western Iran. J Asian Earth Sci 29:859–877

Alavi M (1991) Tectonic map of the Middle East. Geological Survey of Iran, scale 1:2,900,000

Alfred T, Anderson JR (1984) Probable relations between plagioclase zoning and magma dynamics, Fuego Volcano, Guatemala. Am Miner 69:660–676

Allen CM (1991) Local equilibrium of mafic enclaves and granitoids of the Turtle pluton, southeast California: Mineral, chemical and isotopic evidence. Am Miner 76:574–588

Armstrong JT (1988) Quantitative analysis of silicate and oxide minerals: comparison of Monte Carlo, ZAF, and U(qz) procedures. In: Newbury DE (ed) Microbeam analysis-1988. San Francisco Press, San Francisco, pp 239–246

Arth JG (1976) Behavior of trace elements during magmatic processes –a summary of theoretical models and their applications. J Res US Geol Surv 4:41–47

Barbarin B (1991) Enclaves of the Mesozoic calc-alkaline granitoids of the Sierra Nevada Batholith, California. In: Didier J, Barbarin B (eds) Enclaves and granite petrology, developments in petrology 13. Elsevier, Amesterdam, pp 135–153

Barbarin B (2005) Mafic magmatic enclaves and mafic rocks associated with some granitoids of the central Sierra Nevada batholith, California: nature, origin, and relations with the hosts. Lithos 88:155–177

Barbarin B, Didier J (1991) Conclusions: enclaves and granite petrology. In: Didier J, Barbarin B (eds) Enclaves and granite petrology, developments in petrology 13. Elsevier, Amesterdam, pp 545–549

Barbarin B, Didier J (1992) Genesis and evolution of mafic microgranular enclaves through various types of interaction between coexisting felsic and mafic magmas. T Roy Soc Edin-Earth 83:145–153
Bea F (1996) Residence of REE, Y, Th and U in granite and crustal protoliths; implications for the chemistry of crustal melts. J Petrol 37:521–552
Bébien J (1991) Enclaves in plagiogranite of the Guevgueli ophiolitic complex, Macedonia, Greece. In: Didier J, Barbarin B (eds) Enclaves and granite petrology, developments in petrology 13. Elsevier, Amesterdam, pp 205–229
Berberian M, King GCP (1981) Towards a paleogeography and tectonic evolution of Iran. Can J Earth Sci 18:210–265
Blundy JD, Sparks RSJ (1992) Petrogenesis of mafic inclusions in granitoids of the Adamelo Massif, Italy. J Petrol 33:1039–1104
Blundy J, Wood B (2003) Partitioning of trace elements between crystals and melts. Earth Planet Sci Lett 210:383–39
Boynton WV (1984) Cosmochemistry of the rare earth elements: meteorite studies. In: Henderson P (ed) Rare earth element geochemistry. Elsevier, pp 63–114
Castro A, Mereno-Ventas I, De La Rosa JD (1990) Microgranular enclaves as indicators of hybridization processes in granitoid rocks. Hercynian Belt, Spain. Wally Pitcher Conference, University of Liverpool, January 1990. Geol J 25:391–404
Castro A, Moreno-Ventas I, De La Rosa JD (1991) H-type (hybrid) granitoids: a proposed revision of the granite-type classification and nomenclature. Earth Sci 31:237–253
Chappell BW (1978) Granitoids from the Moonbi district, New England Batholith, Eastern Australia. J Geol Soc Aust 25:267–283
Chappell BW (1996) Magma mixing and the production of compositional variation within granite suites: evidence from the granite of Southeastern Australia. J Petrol 37:449–470
Chappell BW, White AJR, Williams IS, Wyborn D, Wyborn LAI (2000) Lachlan Fold Belt granite revisited: high- and low-temperature granite and their implications. Aust J Earth Sci 47:123–138
Chen YD, Price RC, White AJR (1989) Inclusions in three S–type granite from Southeastern Australia. J Petrol 30:1181–1218
Chen B, Chen ZC, Jahn BM (2009) Origin of mafic enclaves from the Taihang Mesozoic orogen, north China craton. Lithos 110:343–358
Clemens JD, Wall VJ (1984) Origin and evolution of a peraluminous silicic ignimbrite suite: the Violet Town Volcanics. Lithos 88:354–371
Clemens JD, Wall VJ (1988) Controls on the mineralogy of S-type volcanic and plutonic rocks. Lithos 21:53–66
Cloos E (1936) Der Sierra-Nevada-pluton in Californien. Neues Jahrb Geol Palaontol-Abh B76:355–450
Dahlquist JA (2002) Mafic microgranular enclaves: early segregation from metaluminous magma (Sierra de Chepes), Pampean Ranges, NW Argentina. J South Am Earth Sci 15:643–655
Didier J (1973) Granite and their enclaves. Elsevier, London
Didier J (1984) The problem of enclaves in granitic rocks, a review of recent ideas on their origin. In: Xu KQ, Tu GC (eds) Geology of granite and their metallogenetic relations, proceedings international symposium, Nanjing, October 1982. Science Press, Beijing, pp 137–144
Didier J, Barbarin B (1991) Enclaves and granite petrology, developments in petrology 13. Elsevier, Amsterdam
Dodge FCW, Kistler RW (1990) Some additional observations on inclusions in the granitic rocks of the Sierra Nevada. J Geophys Res 95:17841–17848
Donaire T, Pascual E, Pin C, Duthou JL (2005) Microgranular enclaves as evidence of rapid cooling in granitoid rocks: the case of the Los Pedroches granodiorite, Iberian Massif, Spain. Contrib Mineral Petrol 149:247–265
Dorais MJ, Whitney JA, Roden MF (1990) Origin of mafic enclaves in the Dinkey Creek Pluton, Central Sierra Nevada batholith, California. J Petrol 31:853–881
Esna-Ashari A, Hassanzadeh J, Wernicke BP, Achmitt AK, Axen G, Horton B (2009) Middle Jurassic flare-up and cretaceous magmatic lull in the central Sanandaj-Sirjan arc, Iran: analogy with the southwestern United States. GSA Annual Meeting, October 2009
Feeley TC, Dungan MA (1996) Compositional and dynamic controls on mafic–silicic interactions at continental arc volcanoes: evidence from Cordon El Guadal, Tatara San Pedro Complex, Chile. J Petrol 37:1547–1577
Feeley TC, Wilson LF, Underwood SJ (2008) Distribution and compositions magmatic inclusions in the Mount Helen dome, Lassen volcanic center, California: insights into magma chamber processes. Lithos 106:173–189
Fershtater GB, Borodina NS (1977) Petrology of autholiths in granitic rocks. Int Geol Rev 19:458–468
Fershtater GB, Borodina NS (1991) Enclaves in the Hercynian granitoids of the Ural Mountains, USSR. In: Didier J, Barbarin B (eds) Enclaves and granite petrology, developments in petrology 13. Elsevier, Amsterdam, pp 83–94
Flinders J, Clemens JD (1995) Non-linear dynamics and the distribution and compositions of enclaves in granitoid magmas. In: Brown M, Piccoli PM (eds) The origin of granite and related rocks. University of Maryland
Fourcade S, Allègre CJ (1981) Trace element behavior in granite genesis: a case study. The calc-alkaline plutonic association from the Quérigut complex (Pyrenees, France). Contrib Mineral Petrol 76:177–195
Frost TP, Mahood GA (1987) Field, chemical and physical constraints on mafic-felsic magma interaction in the Lamark granodiorite, Sierra Nevada, California. Geol Soc Am Bull 99:272–291
Furman T, Spera FJ (1985) Commingling of acid and basic magma with implications for the origin of mafic I-type xenolith: field and petrochemical relations of an unusual dike complex at Eagle Lake, Sequoia National Park, California, USA. J Volcanol Geotherm Res 24:151–178
Gromet LP, Silver LT (1987) REE variations across the Peninsular Ranges Batholith; implications for batholithic petrogenesis and crustal growth in magmatic arcs. J Petrol 28:75–125
Holden P, Halliday AN, Stephens WE, Henney PJ (1991) Chemical and isotopic evidence for major mass transfer between mafic enclaves and felsic magma. Chem Geol 92:135–152
Ilbeyli N, Pearce JA (2005) Petrogenesis of igneous enclaves in plutonic rocks of the Central Anatolian Crystalline Complex, Turkey. Int Geol Rev 47:1011–1034
Keskin M (2002) FC-modeler: a Microsoft Excel spreadsheet program for modeling Rayleigh fractionation vectors in closed magmatic systems. Comput Geosci 28:919–928
Kumar S, Rino V (2006) Mineralogy and geochemistry of microgranular enclaves in Palaeoproterozoic Malanjkhand granitoids, central India: evidence of magma mixing, mingling, and chemical equilibration. Contrib Mineral Petrol 152:591–609
Masoudi F (1997) Contact metamorphism and pegmatite development in the SW of Arak, Iran. Dissertation, University of Leeds
Naney MT, Swanson SE (1980) The effect of Fe and Mg on crystallization in granitic systems. Am Miner 65:639–653
Nash WP, Crecraft HR (1985) Partition coefficients for trace elements in silicic magmas. Geochim Cosmochim Acta 49:2309–2322
Nelson ST, Montana A (1992) Sieve-textured plagioclase in volcanic rocks produced by rapid decompression. Am Miner 77:1242–1249

Pabst A (1928) Observations on inclusions in the granitic rocks of the Sierra Nevada. Univ Calif Publ Geol Sci 17:325–386

Pascual E, Donaire T, Pin C (2008) The significance of microgranular enclaves in assessing the magmatic evolution of a high-level composite batholith: a case on the Los Pedroches Batholith, Iberian Massif, Spain. Geochem J 42:177–198

Pearce JA, Norry MJ (1979) Petrogenetic implications of Ti, Zr, Y and Nb variations in volcanic rocks. Contrib Mineral Petrol 69:33–47

Perugini D, Poli G, Christofides G, Eleftheriadis G (2003) Magma mixing in the Sithonia plutonic complex, Greece: evidence from mafic microgranular enclaves. Mineral Petrol 78:173–200

Petrelli M, Poli G, Perugini D, Peccerillo A (2005) Petrograph: a new software to visualize, model, and present geochemical data in igneous petrology. Geochem Geophys Geosyst. doi:10.1029/2005GC000932

Phillips JA (1880) On concretionary patches and fragments of other rocks contained in granite. J Geol Soc 36:1–21

Phillips GN, Wall VJ, Clemens JD (1981) Petrology of the Strathbogie batholith: a cordierite-bearing granite. Can Mineral 19:47–63

Pin C, Binon M, Belin J, Barbarin B, Clemens JD (1990) Origin of microgranular enclaves in granitoids: equivocal Sr–Nd evidence from Hercynian rocks in the Massif Central (France). J Geophys Res 95:17821–17828

Platevoet B, Bonin B (1991) Enclaves and mafic-felsic associations in the Permian alkaline province of Corsica, France: physical and chemical interactions between coeval magmas. In: Didier J, Barbarin B (eds) Enclaves and granite petrology, developments in petrology 13. Elsevier, Amesterdam, pp 191–204

Romick JD, Kay SM, Kay RM (1992) The influence of amphibole fractionation on the evolution of calc-alkaline andesite and dacite tehpra from the central Aleutians, Alaska. Contrib Mineral Petrol 112:101–118

Ruttner A, Stöcklin J (1967) Geological map of Iran. Geological Survey of Iran, scale 1:1000,000

Sawka WN, Chappell BW (1988) Fractionation of uranium, thorium and rare earth elements in a vertically zoned granodiorite: implications for heat production distributions in the Sierra Nevada batholith, California, U.S.A. Geochim Cosmochim Acta 52:1131–1143

Sengör AMC (1990) A new model for the late Paleozoic–Mesozoic tectonic evolution of Iran and implications for Oman. In: Robertson AHF, Searle MP, Ries AC (eds) The Geology and Tectonics of the Oman Region, Geological Society of London, Special Publication 22, pp 278–281

Shahbazi H, Siebel W, Pourmoafee M, Ghorbani M, Sepahi AA, Shang CK, Vousoughi Abedini M (2010) Geochemistry and U–Pb zircon geochronology of the Alvand plutonic complex in Sanandaj–Sirjan Zone (Iran): New evidence for Jurassic magmatism. J Asian Earth Sci, accepted paper

Silva MMVG, Neiva AMR, Whitehouse MJ (2000) Geochemistry of enclaves and host granite from the Nelas area, central Portugal. Lithos 50:153–170

Singer BS (1993) Plagioclase zoning in mid-Pleistocene lavas from the Seguam volcanic center, central Aleutian arc, Alaska. Am Miner 78:143–157

Stephens WE, Holden P, Henney PJ (1991) Microdioritic enclaves within the Scottish Caledonian granitoids and their significance for crustal magmatism. In: Didier J, Barbarin B (eds) Enclaves and Granite Petrology, Developments in petrology 13. Elsevier, Amesterdam, pp 125–134

Streckeisen AL (1976) To each plutonic rock its proper name. Earth Sci Rev 12:1–34

Tepper JH, Kuehner SM (2003) Geochemistry of mafic enclaves and host granitoids from the Chilliwack batholith, Washintong: chemical exchange processes between coexisting mafic and felsic magmas and implications for the interpretation of enclave chemical traits. J Geol 112:349–367

Troll VR, Donaldson CH, Emeleus CH (2004) Pre-eruptive magma mixing in ash-flow deposits of the Tertiary Rum Igneous Center, Scotland. Contrib Mineral Petrol 147:722–739

Valizadeh MV, Cantagrel JM (1975) Premieres donnees radiometriques (K-Ar et Rb-Sr) sur les micas du complexe magmatique du Mont Alvand pres Hamedan (Iran Occidental). Comptes Rendus Hebdomadares des Seances de l'Academie des Sciences, Serie D, Sciences Naturelles 281:1083–1086

Vernon RH (1983) Restite, xenoliths and microgranitoid enclaves in granite. J Proc R Soc NSW 116:77–103

Vernon RH (1984) Microgranitoid enclaves: globules of hybrid magma quenched in a plutonic environment. Nature 304:438–439

Vernon RH (1990) Crystallization and hybridism in microgranitoid enclave magmas: microstructural evidence. J Geophys Res 95:17849–17859

Vernon RH (1991) Interpretation of microstructures of microgranitoid enclaves. In: Didier J, Barbarin B (eds) Enclaves and granite petrology, developments in petrology 13. Elsevier, Amsterdam, pp 277–291

White AJR, Chappell BW (1977) Ultrametamorphism and granitoid genesis. Tectonophysics 43:7–22

White AJR, Chappell BW, Wyborn D (1999) Application of the restite model to the Deddick granodiorite and its enclaves—a reinterpretation of the observations and data of Maas et al. J Petrol 40:413–421

Wiebe RA (1968) Plagioclase stratigraphy: a record of magmatic conditions and events in a granite stock. Am J Sci 266:690–703

Wiebe RA (1973) Relations between coexisting basaltic and granitic magmas in a composite dike. Am J Sci 273:130–151

Wiebe RA, Smith D, Sturn M, King EM, Seckler MS (1997) Enclaves in the Cadillac mountain granite (Coastal Maine): samples of hybrid magma from the base of the chamber. J Petrol 38:393–423

Wilson M (1989) Igneous petrogenesis: a global tectonic approach. Chapman and Hall, London

Wyllie PJ, Cox KG, Biggar GM (1962) The habit of apatite in synthetic systems and igneous rocks. J Petrol 3:238–243